# Modeling and Control of Offshore Produced Water Treatment Systems Using Online Oil-in-Water Monitors

Jespersen, Stefan

*DOI (link to publication from Publisher):*
10.54337/aau645715783

*Publication date:*
2023

*Document Version*
Publisher's PDF, also known as Version of record

# MODELING AND CONTROL OF OFFSHORE PRODUCED WATER TREATMENT SYSTEMS USING ONLINE OIL-IN-WATER MONITORS

BY
STEFAN JESPERSEN

DISSERTATION SUBMITTED 2023

AALBORG UNIVERSITY
DENMARK

# Modeling and Control of Offshore Produced Water Treatment Systems Using Online Oil-in-Water Monitors

Ph.D. Dissertation

Stefan Jespersen

Dissertation submitted November 13, 2023

Dissertation submitted: November 13, 2023

PhD supervisor:: Associate Professor Zhenyu Yang
Aalborg University

PhD committee: Professor Henrik C. Pedersen
Aalborg University, Denmark
Associate Professor Xuping Zhang
Aarhus University, Denmark
Associate Professor Christian Holden
Norwegian University of Science and Technology, Norway

PhD Series: Faculty of Engineering and Science, Aalborg University

Department: AAU Energy

ISSN (online): 2446-1636
ISBN (online): 978-87-7573-601-0

Published by:
Aalborg University Press
Kroghstræde 3
DK – 9220 Aalborg Ø
Phone: +45 99407140
aauf@forlag.aau.dk
forlag.aau.dk



Printed in Denmark by Stibo Complete, 2023

# Abstract

Oil and gas will remain a vital energy resource while transitioning towards more sustainable and green energy production. Besides the naturally occurring formation water in oil and gas reservoirs, water is often injected to maintain pressure and sweep reservoirs to increase the oil recovery. Produced water (PW) commonly comprises more than 90% of the produced liquid from matured oil fields today, and the PW needs to be cleaned before it is discharged into the ocean. Current Danish regulations require the concentration of oil-in-water (OiW) in PW discharge to be below 30 mg/L and the total annual discharge to be below 222 tonnes. The concentration is measured by taking manual samples, which are sent to a laboratory for testing following the reference method using a gas chromatography-flame ionization detector. In Denmark, online OiW monitors are required to be installed as an additional measurement for reporting as well. These monitors are calibrated using the laboratory-tested manual samples using a reference method. However, current installations do not utilize online OiW monitors for controlling the de-oiling process yet.

Typical offshore installations consist of three-phase gravity separator tanks where the bulk separation of gas, oil, and water occurs as a first-stage separation. In the second separation stage, hydrocyclones are commonly deployed in offshore produced water treatment (PWT) facilities to reduce the OiW concentration before discharge. Current industrial hydrocyclone control solutions utilize the pressure drop ratio (PDR) as the controlled variable with a fixed reference to achieve high steady-state separation efficiency, i.e., low discharge concentration. However, PDR does not directly measure separation efficiency and cannot sense changes in inlet oil concentration or droplet size distribution.

This thesis is dedicated to exploring how online OiW measurements can enhance the control of the water treatment process to reduce the discharge of oil into the marine environment. The OiW monitors can typically only measure part of the crude oil contents depending on the technology, e.g., aromatic oils with UV-fluorescence monitors, and can be sensitive to process operating conditions, sensor fouling, and some chemical substances. There-

fore, the selected fluorescence-based monitors used in this thesis were tested in an experimental facility to evaluate their applicability for feedback control. The monitors were tested under different process conditions to evaluate their accuracy and sensitivity.

The OiW monitors were used to evaluate the performance of three PDR-based controllers: a robust $H_\infty$ controller and a model predictive controller (MPC) as well as the industry standard proportional integral derivative (PID) control solution, while the coupled three-phase separator and hydrocyclone system were subjected to a varying production flow. The $H_\infty$ and MPC achieved similar performances, but the MPC led to the lowest total discharge. Based on the comparison, some potential OiW-based controlled variables were defined.

To design advanced OiW-based controllers, control-oriented models are usually needed. Few models exist in the literature, but they rely on droplet trajectory analysis, which requires the droplet size distribution to be measured online, complicating the model development and the control system implementation. In this thesis, nonlinear polynomial-type Hammerstein-Wiener models are proposed to model the separation dynamics. In particular, models of the separation efficiency, the discharge concentration, and the volumetric discharge rate were identified using the prediction error method on experimental data from a testing facility. The optimal model structure and coefficients were found using an exhaustive search and cross-validation. The models were found to explain the main dynamic and static features of the hydrocyclone separation.

A nonlinear model predictive controller (NMPC) is proposed in this work, which is a cascaded control loop with the NMPC in the outer loop, providing the reference to the PID-type PDR controller in the inner loop. The developed controller optimizes the dynamic separation efficiency, which resulted in a significant improvement compared with the standard PID controller alone without negatively impacting oil production. In principle, this could be extended with control of the separator level to achieve even better separation performance while rejecting changes in production rate.

In conclusion, this thesis developed a methodology to identify control-oriented models of hydrocyclones using OiW concentration data and a potential solution to implementing OiW-based control that combines the advantages of both the OiW measurements and the traditional PDR-based approach.

# Resumé

Olie og gas vil fortsat være en vigtig energiressource under transitionen mod en mere bæredygtige og grønnere energiproduktion. Udover det naturligt forekomne formationsvand injiceres vand ofte ind i oile og gas reservoirer for at opretholde trykket og øge olieindvindingen. Produceret vand udgør ofte mere end 90 % af den producerede væske fra modne oliefelter, som skal renses før det bliver udledt til havet. Den nuværende danske lovgivning kræver at koncentrationen af olie i det producerede vand reduceres til under 30 mg/L og at den totale olieudledning i den danske sektor holdes under 222 ton. Koncentrationen måles ved at tage manuelle prøver som sendes til et laboratorie hvor de testes ved brug af en referencemetode, som benytter en gaskromatografi flammeioniseringsdetektor. I Danmark er det et krav at der installeres online målere til bestemmelse af koncentrationen af olie i vand som en ekstra måling til rapportering af olieudledningen. Disse målere kalibreres ved hjælp af manuelle prøver og den pågældende reference metode. Nuværende vandbehandlingsanlæg udnytter dog endnu ikke de online oliekoncentrationsmålinger til at kontrollere separationsprocessen.

Offshore installationer består typisk af separator tanke hvor størstedelen af separationen af gas, olie og vand sker, som det første stadie. I andet separationsstadie anvendes der ofte hydrocycloner for at reducere oliekoncentrationen yderligere før vandet udledes til havet. Nuværende industrielle hydrocyklon kontrol løsninger er baseret på trykdifferensforholdet (PDR) som den kontrollerede variabel med en konstant reference for at opnå høj separationseffektivitet og dermed lav oliekoncentration i udledningen. Men da PDR ikke er en direkte måling af separationseffektiviteten kan ændringer i oliekoncentrationer eller størrelsen af oliedråber ikke registered.

Denne afhandling er dedikeret til at undersøge hvordan online målinger af olie i vand kan forbedre kontrollen af behandlingsanlæg til produceret vand og derved reducere udledningen af olie til havet. Afhængigt af den pågældende teknologi, måler online oliekoncentrationsmålere typisk kun på en del af råolien, som f.eks. aromatisk olie for UV-fluorescens målere og de kan være følsomme overfor operationsforhold. Derfor blev der foretaget tests af de udvalgte fluorescensbaserede målere i et eksperimentelt anlæg for at

evaluere deres egnethed som sensorer i et kontrolsystem. Målerne blev testet under forskellige procesforhold for at evaluere deres nøjagtighed samt sensitivitet. De online oliekoncentrationsmålere blev anvendt til at evaluere ydeevnen af tre PDR baserede kontrollere: robust $H_\infty$ control, model prædiktiv kontrol (MPC) og konventionel proportional integral differential (PID) kontrol mens det kombinerede system bestående af en separator tank og en hydrocyklon, blev udsat for varierende produktion. Anvendelsen af $H_\infty$ og MPC resulterede i lignende ydeevne, men brugen af MPC ledte til den laveste totale olieudledning. Baseret på sammenligningen blev der defineret nogle potentielle kontrollerede variable.

For at designe avancerede kontrollere baseret på oliekoncentrationsmålinger, er der ofte brug for en kontrol-orienteret model. Der findes enkelte modeller, men de er ofte baseret på analyse af oliedråbernes banekurver, hvilket nødvendiggør online målinger af dråbestørrelsesfordelingen, som komplicerer udviklingen af modeller samt implementeringen af kontrolsystemet. I denne afhandling, foreslås polynomiumbaserede Hammerstein-Wiener modeller til at repræsentere separationsdynamikken. Modeller af separationseffektiviteten, udledningskoncentrationen, og den volumetriske udledningsrate blev identificeret ved brug af prædiktionsfejlsmetoden på eksperimentelle data fra et testanlæg. Den optimale modelstruktur of koefficienter blev fundet ved brug af en udtømmende søgning og brug af krydsvalidering. Det blev vurderet at modellerne forklarer den installerede hydrocyklons dynamiske og statiske egenskaber i en tilstrækkelig grad.

Det foreslås at bruge en nonlineær model prædiktiv kontrol (NMPC) i kaskade med den eksisterende PDR kontrolsløjfe, med NMPC'en i den ydre sløjfe der bestemmer referencen til PID-kontrolleren der styrer PDR i den indre sløjfe. NMPC'en optimerer den dynamiske separationseffektivitet, hvilket resulterede i en signifikant forbedring sammenlignet med den eksisterende PID-baserede kontrol, uden at påvirke olieproduktionen negativt. Denne løsning kan principielt udvides til også at styre vandniveauet i separator tanken for at opnå endnu bedre separationsydeevne og samtidig mitigere forstyrrelserne fra den varierende production.

I denne afhandling blev der udviklet en fremgangsmåde til at identificere kontrolorienterede modeller af hydrocykloner baseret på oliekoncentrationsmålinger og en potentiel løsning til implementering af oliekoncentrationsbaseret control blev foreslået som kombinerer fordelene ved både oliekoncentrationsmålingerne samt den traditionelle PDR baserede fremgangsmåde.

# Contents

**Abstract** iii

**Resumé** v

**Thesis Details** ix

**Preface** xiii

**Abbreviations** xv

**I Extended Summary** 1

**1 Introduction and Motivation** 3
1.1 Background . . . 5
1.1.1 Three-Phase Gravity Separators . . . 6
1.1.2 Hydrocyclones . . . 7
1.1.3 Control Strategy . . . 10
1.1.4 Oil-in-Water Monitoring . . . 12
1.2 Motivation for Control based on Online Oil-in-Water Monitors 14
1.2.1 Motivation for Hydrocyclone Modeling . . . 15
1.3 Outline of the Papers . . . 15
1.3.1 Motivation for Paper A . . . 16
1.3.2 Motivation for Paper B . . . 17
1.3.3 Motivation for Paper C and D . . . 17
1.3.4 Motivation for Paper E . . . 18

**2 Preparation for Online Oil-in-Water Monitoring** 19
2.1 Produced Water Treatment Testing Facility . . . 19
2.2 Calibration and Challenges of UV-Fluorescence Monitors . . . 21
2.2.1 UV-Fluorescence Monitor Challenges . . . 23
2.2.2 Testing Facility Related Challenges . . . 25
2.3 Oil-in-Water Monitor Sidestream Upgrade . . . 27

2.4 Conclusion . . . . . 29

**3 Performance Evaluation of Pressure Drop Ratio Control Using Oil-in-Water Monitors 31**
3.1 Models of Separator Level and Hydrocyclone Pressure Drop Ratio . . . . . 32
3.2 Pressure Drop Ratio Control Solutions . . . . . 33
3.3 Performance Evaluation of Pressure Drop Ratio Control . . . . 35
3.4 Conclusion . . . . . 40

**4 Modeling of Oil-in-Water Separation Dynamics 41**
4.1 Hammerstein–Wiener Nonlinear Model Structure and Identification Approach . . . . . 42
4.1.1 System Identification Results . . . . . 44
4.2 Conclusion . . . . . 47

**5 Control Based on Online Oil-in-Water Measurements 49**
5.1 Skogestad Internal Model Control . . . . . 49
5.2 Nonlinear Model Predictive Control . . . . . 51
5.3 Conclusion . . . . . 53

**6 Closing remarks 55**
References . . . . . 58

**II Papers 65**

**A Flow-Loop Testing of Online Oil-in-Water UV-Fluorescence-Based Measurement 67**

**B Performance Evaluation of a De-oiling Process Controlled by PID, $H_\infty$ and MPC 77**

**C Hammerstein-Wiener Model Identification of De-oiling Hydrocyclone Separation Efficiency 85**

**D Hammerstein–Wiener Model Identification for Oil-in-Water Separation Dynamics in a De-Oiling Hydrocyclone System 93**

**E Nonlinear Model Predictive Control of Hydrocyclone Separation Efficiency 127**

# Thesis Details

| | |
|---|---|
| **Thesis Title:** | Modeling and Control of Offshore Produced Water Treatment Systems Using Online Oil-in-Water Monitors |
| **Ph.D. Student:** | Stefan Jespersen |
| **Supervisor:** | Associate Prof. Zhenyu Yang, Aalborg University, DK |

The body of the thesis consists of the following papers:

**[A]** S. Jespersen, D. S. Hansen, Z. Yang, and S. I. Andersen, "Flow-Loop Testing of Online Oil-in-Water UV-Fluorescence-Based Measurement," in Proceedings of *the 2nd International Conference on Signal, Control and Communication (SCC)*. Hammamet, Tunisia: IEEE, 20–22 Dec. 2021, pp. 313–319. Doi: 10.1109/SCC53769.2021.9768363

**[B]** S. Jespersen, and Z. Yang, "Performance Evaluation of a De-oiling Process Controlled by PID, $H_\infty$ and MPC," in Proceedings of *IECON 2021 - 47th Annual Conference of the IEEE Industrial Electronics Society*. Toronto, ON, Canada: IEEE, 13–16 Oct. 2021, pp. 1–6. Doi: 10.1109/IECON48115.2021.9589250

**[C]** S. Jespersen, M. Kashani, and Z. Yang, "Hammerstein-Wiener Model Identification of De-oiling Hydrocyclone Separation Efficiency," in Proceedings of *the 9th International Proceedings of Conference on Control, Decision and Information Technologies (CoDIT)*. Rome, Italy: IEEE, 3–6 Jul. 2023, pp. 2508–2513. Doi: 10.1109/CoDIT58514.2023.10284508

**[D]** S. Jespersen, Z. Yang, D. S. Hansen, M. Kashani and Biao Huang, "Hammerstein–Wiener Model Identification for Oil-in-Water Separation Dynamics in a De-Oiling Hydrocyclone System," *Energies*, MDPI, vol. 16, no. 20, pp. 1–33, 2023. Doi: 10.3390/en16207095

**[E]** S. Jespersen, D. S. Hansen, M. V. Bram, M. Kashani, and Z. Yang, "Nonlinear Model Predictive Control of Hydrocyclone Separation

Efficiency," in Proceedings of *the 12th IFAC Symposium on Advanced Control of Chemical Processes (ADCHEM)*. Toronto, ON, Canada: IFAC, 14–17 Jul. 2024, pp. 1–6. [Submitted for publication]

In addition, the following publications have also been co-authored:

**[1]** D. Hansen, M. Bram, P. Durdevic, S. Jespersen, and Z. Yang, "Efficiency evaluation of offshore deoiling applications utilizing real-time oil-in-water monitors," in Proceedings of *Oceans 2017 - Anchorage*. Anchorage, AK, USA: IEEE, 18–21 Sep. 2017, pp. 1–6. Available: https://ieeexplore.ieee.org/document/8232154

**[2]** E. K. Nielsen, S. Jespersen, X. Zhang, O. Ravn, and M. Lind, "Online Fault Diagnosis of Produced Water Treatment with Multilevel Flow Modeling," *IFAC-PapersOnLine*, Elsevier, vol. 51, no. 8, pp. 225–232, 2018. Doi: 10.1016/j.ifacol.2018.06.381

**[3]** D. S. Hansen, S. Jespersen, M. V. Bram, and Z. Yang, "Human Machine Interface Prototyping and Application for Advanced Control of Offshore Topside Separation Processes," in Proceedings of *IECON 2018 - 44th Annual Conference of the IEEE Industrial Electronics Society*. Washington, DC, USA: IEEE, 21–23 Oct. 2018, pp. 2341–2347. Doi: 10.1109/IECON.2018.8591309

**[4]** D. S. Hansen, S. Jespersen, M. V. Bram, and Z. Yang, "Uncertainty Analysis of Fluorescence-Based Oil-In-Water Monitors for Oil and Gas Produced Water," *Sensors*, MDPI, vol. 20, no. 16, pp. 1–36, 2020. Doi: 10.3390/s20164435

**[5]** M. V. Bram, S. Jespersen, D. S. Hansen, and Z. Yang, "Control-Oriented Modeling and Experimental Validation of a Deoiling Hydrocyclone System," *Processes*, MDPI, vol. 8, no. 9, pp. 1–33, 2020. Doi: 10.3390/pr8091010

**[6]** D. S. Hansen, S. Jespersen, M. V. Bram, and Z. Yang, "Offshore Online Measurements of Total Suspended Solids using Microscopy Analyzers," *Sensors*, MDPI, vol. 21, no. 9, pp. 1–19, 2021. Doi: 10.3390/s21093192

**[7]** L. C. Igbokwe, G. F. Naterer, S. Zendehboudi, S. Pedersen, and S. Jespersen, "Suppression of liquid slugs and phase separation through pipeline bends," *The Canadian Journal of Chemical Engineering*, Wiley, vol. 100, no. 8, pp. 1778–1795, 2020. Doi: 10.1002/cjce.24289

**[8]** M. Kashani, S. Jespersen, and Z. Yang, "Robust Multivariable Model Reference Adaptive State Feedback Output Tracking Control: An Offshore Produced Water Treatment Case Study," in Proceedings of *the 9th International Conference on Control, Decision and Information Technologies (CoDIT)*. Rome, Italy: IEEE, 3–6 Jul. 2023, pp. 2317–2324. Doi: 10.1109/CoDIT58514.2023.10284220

**[9]** M. Kashani, S. Jespersen, and Z. Yang, "Robust Adaptive Control of Offshore Produced Water Treatment Process: An Improved Multivariable MRAC-Based Approach," *Journal of Process Control*, Elsevier, pp. 1–27, 2023. [Submitted for publication]

**[10]** M. Kashani, S. Jespersen, and Z. Yang, "Impact of System Initial Values on Multivariate LSTM Neural Network Performance: A Finding From a Control Process Perspective" in Proceedings of *the 11th International Conference on Control, Mechatronics and Automation (ICCMA 2023)*. Grimstad, Norway: IEEE, 1–3 Nov. 2023, pp. 1–6. [Accepted/In press]

**[11]** K. F. Pajuro, L. B. Hansen, M. K. Odena, S. Jespersen, Z. Yang, "Modelling the Oil-in-Water Separation Dynamics in a De-Oiling Hydrocyclone System Using LSTM Neural Network," in Proceedings of *the 49th Annual Conference of the IEEE Industrial Electronics Society (IECON 2023)*. Singapore, Republic of Singapore: IEEE, 16–19 Oct. 2023, pp. 1–6. [Accepted/In press]

**[12]** Z. Yang, S. Jespersen, D. S. Hansen, K. F. Pajuro, F. Liu, J. Vollertsen, "Capturing Microplastics from Aquatic Systems Using Vortex based Cyclone Technique," in Proceedings of *the 18th International Conference on Environmental Science and Technology (CEST 2023)*. Athens, Greece: 30–31 Aug. & 1–2 Sep. 2023, pp. 1–4. [Accepted/In press]

This thesis has been submitted for assessment in partial fulfillment of the Ph.D. degree. The thesis is based on the submitted or published scientific papers that are listed above. The thesis's body consists directly of papers A–E, where papers 1–12 are additional papers related to offshore oil and gas. As part of the assessment, co-author statements have been made available to the assessment committee and available at the faculty. The thesis is not acceptable for open publication in its present form but only in limited and closed circulation, as copyright may not be ensured.

# Preface

This thesis is submitted as a collection of papers to fulfill the requirements for the degree of Doctor of Philosophy at AAU Energy, Aalborg University, Denmark. The work was carried out in AAU Energy, Aalborg University, Esbjerg Campus, in the period from August 2020 to November 2023, under the supervision of Associate Professor Zhenyu Yang. During the project period, I was a visiting researcher in the Department of Chemical and Materials Engineering at the University of Alberta from July 2022 to November 2022 under the supervision of Professor Biao Huang. The project has been supported by the Danish Offshore Technology Centre and Aalborg University joint project: "MPC: Model predictive control for slug flow suppression, Aalborg University, Pr-no: 222590".

I would like to thank all my colleagues from AAU Energy for providing a pleasant and friendly research environment. I would like to thank my supervisor, Zhenyu Yang, for his constant positive support and encouragement, for all our valuable discussions, and for being a friend. I would also like to thank Professor Biao Huang and his talented research team for an inspiring stay at Alberta University. A special thanks to my brilliant colleagues and friends, Dennis Severin Hansen and Mads Valentin Bram, for valuable discussions and for always being there when I needed help.

In addition, I would like to thank my family and friends, and especially my fiance, for endlessly supporting me through tough and difficult times.

Stefan Jespersen
Aalborg University, November 13, 2023

# Abbreviations

| | |
|---|---|
| BTEX | Benzene, toluene, ethylbenzene, and xylenes |
| CFD | Computational fluid dynamics |
| EIA | Energy Information Administration |
| GC-FID | Gas chromatography-flame ionization detector |
| HW | Hammerstein-Wiener |
| IEA | International Energy Agency |
| LFT | Linear fractional transformation |
| MIMO | Multiple-input multiple-output |
| MISO | Multiple-input single-output |
| MPC | Model predictive control |
| NMPC | Nonlinear model predictive control |
| NRMSE | Normalized root mean square error |
| OiW | Oil-in-water |
| OLS | Ordinary least square |
| OSPAR | Oslo and Paris |
| PDR | Pressure drop ratio |
| PID | Proportional integral derivative |
| ppm | Parts per million |
| PW | Produced water |
| PWT | Produced water treatment |

| | |
|---|---|
| RFU | Raw fluorescence unit |
| SAE | Society of Automotive Engineers |
| SIMC | Skogestad internal model control |
| TF | Transfer function |
| UV | Ultraviolet |
| WLS | Weighted least square |

# Part I

# Extended Summary

# Chapter 1

# Introduction and Motivation

The global energy demand is expected to increase from 673 exajoules in 2022 to 902 exajoules in 2050, primarily due to the increasing population and improving living standards [1]. Despite a significant and increasing amount of energy from renewable sources, the Energy Information Administration (EIA) projects that global oil production will increase for the next 30 years. Energy security concerns are likely to expedite the transition towards renewable energy in some countries but lead to increased fossil fuel consumption in others [1]. Other agencies have made similar projections to 2050, like the International Energy Agency (IEA), which presents three scenarios. With the currently implemented policies, global oil production is expected to increase by approximately 10% from 90.3 million barrels per day (mb/d) in 2021 to 99.3 mb/d by 2050. In the second scenario, all targets announced by governments are met, including their long-term net zero goals, resulting in a 39% reduction in global oil production by 2050 to 55.3 mb/d. In a scenario with net zero emissions achieved by 2050, global oil production is estimated to be reduced by about 75% to 22.2 mb/d. In all projected cases, whether it is IEA or EIA, the global oil production will likely remain substantial until 2050 and beyond [2].

Today, about 70% of the produced oil comes from mature fields there is more than 30 years old and, thus, have passed their production peak. This raises the attention on maximizing the recovery factor from mature fields meanwhile protecting the environment [3]. Of the world's oil production, the offshore industry accounts for about 25-30% today [2]. The production of hydrocarbons relies on the underground reservoir pressure, pushing the mixture of oil, gas, and water into the production facility. Enhanced recovery methods are applied to increase oil production over the lifetime of the hydrocarbon reservoir, such as the injection of water, steam, gases, or chemicals. Water injection is commonly used to maintain reservoir pressure and

sweep the oil through the reservoir to the production wells. In the Danish part of the North Sea, producers have injected water into the reservoirs since 1986 to such an extent that water accounts for about 90% of the extracted liquid volume, see Fig. 1.1. While the water cut continually increases, Danish oil production peaked in 2004 and has been declining ever since, which resulted in Denmark being a net importer of oil since 2018 to meet the energy demand [4]. While some countries, including Denmark, plan to end oil production by 2050, considerable amounts of oil will be produced over the remaining years and likely continue in other parts of the world.

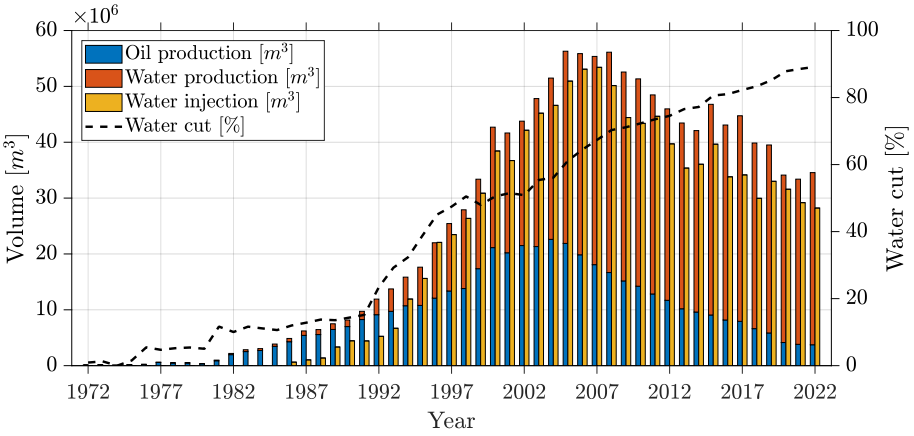


**Fig. 1.1:** The volume of produced oil and water and the amount of injected water in the Danish sector of the North Sea between 1972 and 2022. The dashed line indicates the fraction of water to the total produced liquid volume. The data are published annually by the Danish Energy Agency [5].

The increased volumes of produced water (PW), which need to be processed to maintain production, put strain on the water treatment processes. The PW undergoes several cleaning stages, but it still contains residuals of oil that may harm the marine environment [6]. National laws and regional regulations govern the allowable discharge concentration and quantity. The Oslo and Paris (OSPAR) commission is a regional sea convention established to protect the marine environment of the North East Atlantic. Contracting parties of OSPAR must implement regulations concerning the discharge of PW. In particular, the discharge concentration for each installation must be below 30 mg/L, taken as a monthly average based on at least 16 manual samples. The oil-in-water (OiW) concentration in the samples is measured with the current OSPAR reference method, a lab-based method using a gas chromatography analyzer with a flame ionization detector gas chromatography-flame ionization detector (GC-FID) [7]. Although most oil and gas installations complied with the discharge concentration limit on average, the annual

hydrocarbon discharge in the North Sea amounted to 4000 tonnes between 2009 and 2019 [8].

Based on a recommendation from OSPAR, the Danish Environmental Protection Agency established a reduction target of 222 tonnes of discharged oil annually, which was first met in 2010 and has since been kept a requirement. Each operator in the Danish sector of the North Sea must apply for discharge permission and is then assigned a fraction of the 222 tonnes as an upper annual limit of discharge quantity. For instance, the total discharge limit for TotalEnergies, former Total, was 202 tonnes in 2019 [9]. The increasing amount of PW makes it difficult for the operators to comply with the discharge limits, e.g., the total discharge in 2016 reached 200 tonnes [10]. With the increased focus on the environmental impact of industrial activities, the legislation tends to become stricter. As such, the environmental argument for OiW monitoring and reducing discharges is as strong as the economic one [11]. Some oil and gas operators choose to re-inject the PW to stay below the discharge limit, but sufficient water quality must still be kept to avoid formation damage in the reservoir. PW re-injection with residual oil content has been shown to affect the injectivity, and several experiments indicate that oil droplets smaller than the pore throat diameter decrease the permeability of the reservoir [12, 13]. Thus, improving the produced water treatment (PWT) would reduce the environmental impact of oil and gas production if the PW is discharged or increase the oil production if the PW is re-injected. As a national regulation, the Danish Environmental Protection Agency requires producers to install online OiW monitors and flowmeters to quantify the discharge volume. Although the OiW monitors are installed and sometimes used for process optimization by examining the trend, they are not directly used to control the separation process. This raises the question:

> *"Can online OiW monitors be used to improve the separation performance of the produced water treatment systems?"*

## 1.1 Background

A typical offshore PWT system includes separator tanks and de-oiling hydrocyclones as illustrated in Fig. 1.2 [14–17]. The first separation stage in the PWT system commonly consists of a three-phase separator tank to separate the oil from the gas and water. As the water outlet still contains small oil droplets after the separator tank, which is due to the limited residence time, a second stage of PW separation occurs in the hydrocyclone, which reduces the OiW concentration further. The separated oil-rich mixture is typically reprocessed and eventually becomes a part of the oil production. The cleaned PW after the second stage purification is discharged if it meets the discharge regulations or is re-injected into the reservoir.

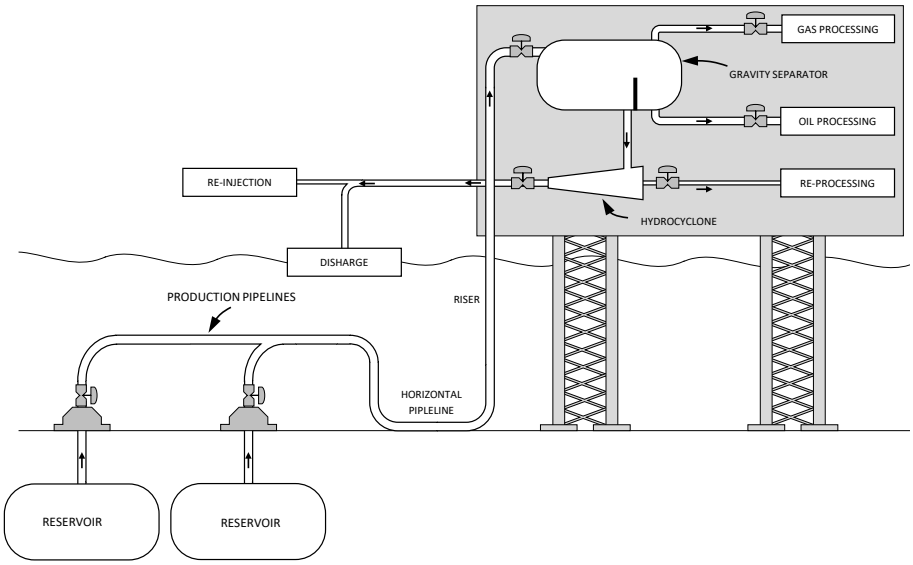


**Fig. 1.2:** A simplified overview of the offshore oil and gas production and produced water treatment (PWT) process.

### 1.1.1 Three-Phase Gravity Separators

The produced liquid and gas mixture enters the three-phase gravity separator tank through the top-side choke valve denoted by $V_{topside}$ in Fig. 1.3. The water, oil, and gas are separated due to their density difference, with the gas rising to the top of the separator tank and the oil droplets settling on the water surface, creating a water-oil interface. The oil layer is separated from the water by letting it flow over a weir into the oil chamber, as shown on the right in Fig. 1.3. Oil and gas exit the separator tank through outlets with the control valves, $V_{oil}$, and $V_{gas}$, respectively. The separation of oil droplets in the three-phase separator tank can be described by Stokes law, which describes the terminal velocity of an oil droplet [18,19]

$$V_t = \frac{D^2(\rho_{oil} - \rho_{water})g}{18\mu}, \tag{1.1}$$

where D is the droplet diameter, g is the gravitational constant, $\mu$ is the viscosity of the continuous phase (here water), and $\rho_{water}$ and $\rho_{oil}$ are the densities of water and the oil, respectively. From equation 1.1, smaller droplets will reach a lower terminal velocity and, consequently, take a longer time to separate. Thus, better separation can be achieved by increasing the residence time, which increases the chance of droplets reaching the water-oil interface before exiting the water outlet. On the other hand, as the size of the separator

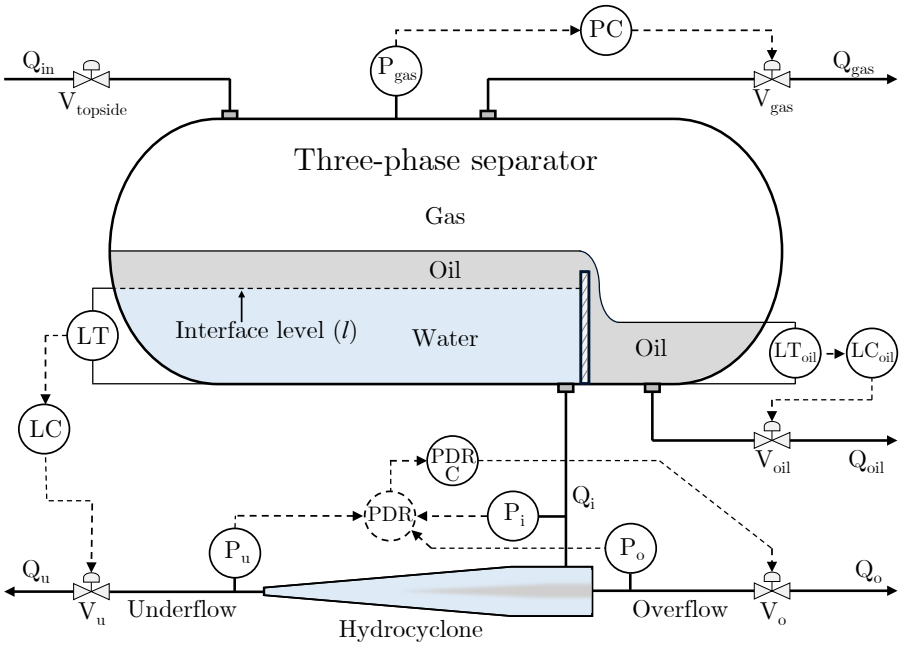


**Fig. 1.3:** Simplified overview of the PWT system, consisting of the coupled three-phase separator tank and hydrocyclone system with water-oil interface level controller LC, oil level controller $LC_{oil}$, pressure drop ratio (PDR) controller PDRC and separator pressure controller PC.

is limited by space and weight constraints, a larger residence time offshore means lower throughput and, therefore, reduced production. The operation of a three-phase separator is, therefore, a trade-off between throughput and separation performance. The control objective of the separator tank is to keep the water-oil interface level below the top of the weir plate to keep water from entering the oil chamber and keep the interface level above a minimum level to keep the oil layer from entering the water outlet.

### 1.1.2 Hydrocyclones

Hydrocyclones were first used in the mining and mineral industry to separate solids from liquids during the late 1800s. The research of hydrocyclones for liquid-liquid separation was initiated in 1968, and the offshore oil and gas industry adopted hydrocyclones for PWT in the 1980s due to the need for compact separation technology [20, 21]. The advantages of the hydrocyclone are small installation footprint, low investment and maintenance cost, and large throughput compared with other separation technologies such as gas flotation and membrane filtration [22]. The hydrocyclone is typically ca-

pable of separating oil droplets as low as 10-15 microns [23]. A simplified illustration of a hydrocyclone liner is shown in Fig. 1.4.

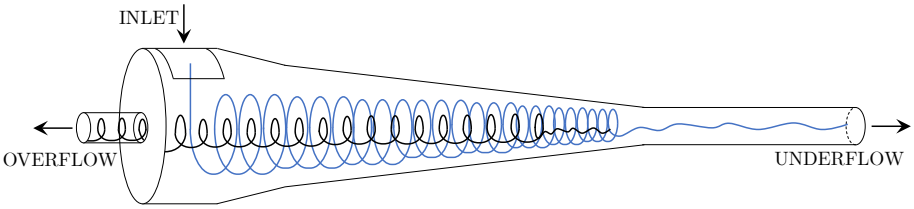


**Fig. 1.4:** Simplified illustration of the vortex flow inside a hydrocyclone liner. The separated oil is rejected through the overflow, while the PW discharge exits through the underflow [24].

The liquid mixture enters the first cylindrical section tangentially to the wall, generating a rotating flow. The conical sections accelerate the liquid due to the decreasing diameter, and a large centripetal acceleration is generated, which separates the oil and water due to their density difference. The dense liquids, i.e., water, are forced to the cyclone wall, while the lighter oil will migrate towards the center of the vortex [25–28]. The cleaned PW leaves the underflow, while the separated oily water leaves through the overflow.

Similar to the three-phase separator, the terminal velocity of the oil droplets can be described by Stokes's law

$$V_t = \frac{D^2(\rho_{oil} - \rho_{water})(V^2/r)}{18\mu}, \tag{1.2}$$

where $V$ is the tangential velocity of the oil droplet and $r$ is the radial position of the droplet from the hydrocyclone center axis. Thus, the gravitational constant in (1.1) is replaced by the centripetal acceleration $(V^2/r)$ acting on the droplets due to the vortex flow. For a hydrocyclone placed horizontally, gravitation will have an effect, but it is typically negligible compared with the centripetal acceleration, which can be as high as 2000-3000g [14, 27].

The hydrocyclone separation efficiency can be defined as the ratio of the volume of separated oil to the volume of oil entering the hydrocyclone, also referred to as the oil removal efficiency

$$\varepsilon_{oil} = \frac{Q_o C_o}{Q_i C_i} = 1 - \frac{Q_u C_u}{Q_i C_i}, \tag{1.3}$$

where $C_i$, $C_o$, and $C_u$ are the inlet, overflow, and underflow volumetric OiW concentration, while $Q_i$ and $Q_u$ are the inlet flow rate and underflow flow rate, respectively. Since $Q_i \approx Q_u$, the oil removal efficiency can be approximated by the oil concentration-reducing separation efficiency defined as [29–31]

$$\varepsilon_{red} = 1 - \frac{C_u}{C_i}. \tag{1.4}$$

Increasing the inlet flow rate $Q_i$ increases the centripetal forces exerted on the fluid, which enhances the separation but simultaneously reduces the residence time and causes oil droplet break-up due to increased shearing forces on the droplets [32]. The steady-state separation efficiency, therefore, increases with the inlet flow rate ($Q_i$) but reaches a plateau above a certain flow rate $Q_{min}$ as illustrated in Fig. 1.5.

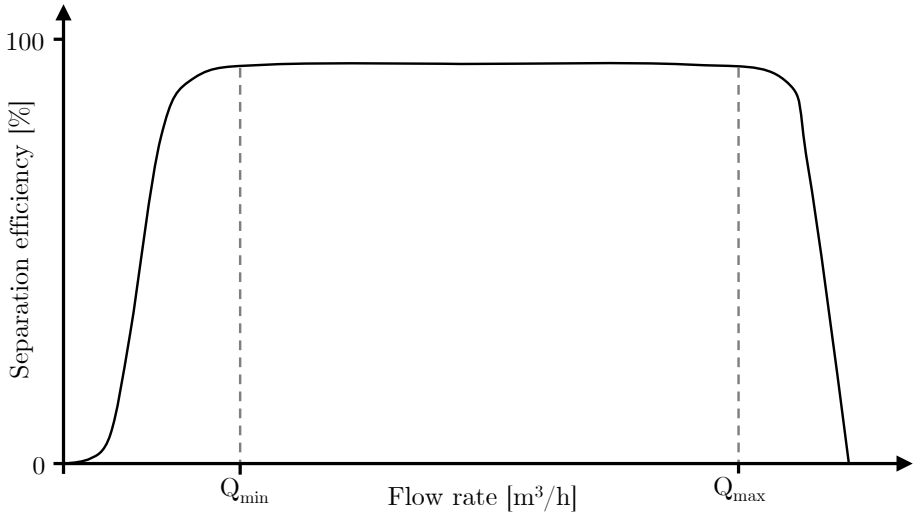


**Fig. 1.5:** Relationship between inlet flow rate $Q_i$ and separation efficiency, with a efficiency plateau between $Q_{min}$ and $Q_{max}$ [32–35].

The efficiency eventually deteriorates as $Q_i$ continues to increase due to droplet break-up or lack of sufficient pressure gradient to force the oil core through the overflow [33,34]. The range of flow rates between $Q_{min}$ and $Q_{max}$ with high steady-state separation efficiency depends highly on the geometric body of the hydrocyclone. The separation efficiency is also dependent on the flow split $F_s$ defined as the ratio of the overflow flow rate $Q_o$ to the inlet flow rate $Q_i$

$$F_s = \frac{Q_o}{Q_i} \approx \frac{Q_o}{Q_u}. \tag{1.5}$$

A general hydrocyclone's relationship between $F_s$ and separation efficiency is illustrated in Fig. 1.6. The steady-state separation efficiency has empirically been found to become essentially constant above a $F_s$ of 2% [29, 33], and others have even documented a high efficiency measured at a $F_s$ of 1% [32]. This relationship has been shown to remain constant within $Q_{min}$ and $Q_{max}$. Increasing the flow split further increases the fraction of water separated from the oil, which constitutes additional operational costs as the water has to be reprocessed.

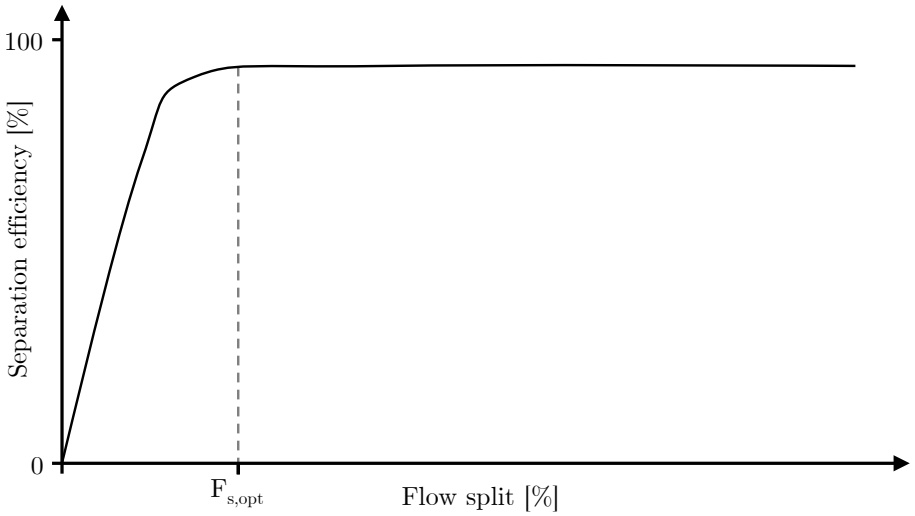


**Fig. 1.6:** Expected relationship between flow split $F_s$ and separation efficiency for flow rates between $Q_{min}$ and $Q_{max}$ in Fig. 1.5. $F_{s,opt}$ represents the optimum flow split [32–35].

The observations in Fig. 1.5 and Fig. 1.6 form the basis for the conventional control strategy implemented offshore. As implied by (1.2), the separation efficiency $\varepsilon$ additionally depends on the oil characteristics, droplet size distribution as well as the inlet concentration $C_i$ [27, 33, 36, 37].

### 1.1.3 Control Strategy

The conventional control strategy offshore of the coupled separator tank and hydrocyclone system is based on a proportional integral derivative (PID) controller for the level in the separator tank and another independently working PID controller for the pressure drop ratio (PDR) of the hydrocyclone, as illustrated in Fig. 1.3. PDR is typically used instead of measuring flow split directly and is defined as

$$PDR = \frac{\Delta P_{io}}{\Delta P_{iu}} = \frac{P_i - P_o}{P_i - P_u}, \tag{1.6}$$

where $P_i$, $P_o$, and $P_u$ are the inlet, overflow, and underflow pressures, respectively. PDR has been shown to be positively correlated with flow split, which makes the PDR a reasonable intermediate variable [32, 33]. The PDR reference is typically 2–3, which is often determined empirically [32].

The level in the separator tank is measured by the level transmitter (LT), and the level controller (LC) actuates the underflow valve $V_u$ of the hydrocyclone system, which sends flow $Q_i$ into the hydrocyclone to keep the level at a specific reference. The PDR controller actuates the overflow valve $V_o$ of the

hydrocyclone system to indirectly keep a high separation efficiency within the hydrocyclone.

The performance of the two control systems is heavily dependent on each other due to the physical coupling of the system. This is illustrated in Fig. 1.7, which shows the typical control structure offshore. Fluctuations in the production flow $Q_{in}$ act as disturbance into the three-phase separator tank, affecting both the subsystems, as the oscillating $Q_{in}$ will impact the level inside the separator tank, triggering the level controller to maintain the given reference by manipulating $V_u$. This will consequently influence flow condition $Q_i$ into the hydrocyclone subsystem that actuates $V_o$ to maintain a given PDR value to keep a certain separation efficiency within the hydrocyclone.

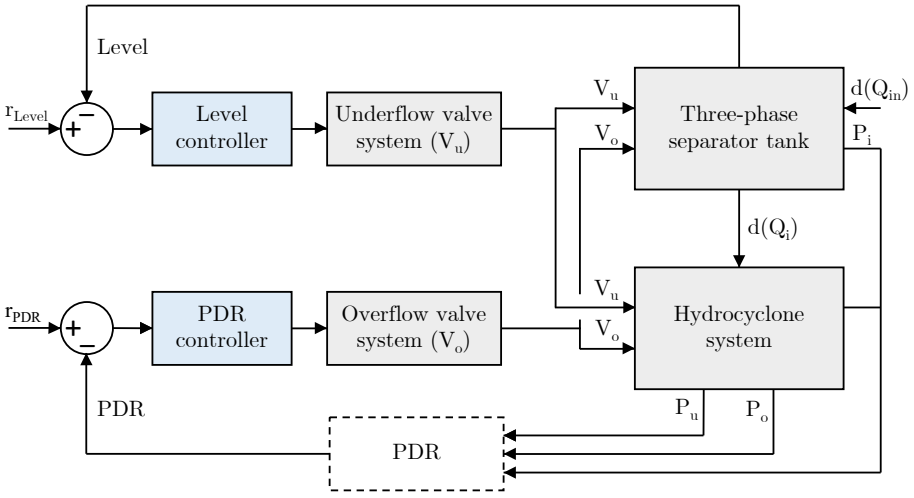


**Fig. 1.7:** Block diagram of the typical control of PWT systems, depicting the inherent coupling in the system.

Some observed issues and challenges with the current operational control strategy can be summarized as:

- Hydrocyclone separation efficiency depends strongly on the inlet flow rate $Q_i$, in some operating ranges, which is determined by the opening degree of $V_u$ commanded by the level controller [32,38,39].
- With an aggressive level controller, variations in the separator tank's inlet flow rate $Q_{in}$ are propagated downstream and turn into variations in hydrocyclone inlet flow rate $Q_i$. Additionally, a low production flow rate $Q_{in}$ can cause $V_u$ to become fully closed, resulting in poor separation [32,38–40].
- PDR depends strongly on $V_u$, which can make the PDR controller saturate $V_o$, leading to either high discharge concentration or high water

content in the separated oil [38, 40].

- The oil-water level controller is designed to keep a fixed level $l$. However, this is not necessary as long as $l$ is kept within a safety range [40].

The listed issues are related to the interconnected system being controlled by independently tuned PID controllers. Solutions to these problems have been investigated by implementing advanced multiple-input multiple-output (MIMO) controllers such as model predictive control (MPC) and $H_\infty$ control [40, 41]. The PDR-based control has been used to control the hydrocyclone due to the reliability of pressure measurements and the lack of reliable online measurements of the OiW concentration in the past. However, some limitations of the use of PDR are:

- PDR and $\varepsilon_{oil}$ are uncorrelated in some operating conditions [38, 42, 43].
- While the PDR control loop can control the flow split and respond to changes in $Q_i$, it is unable to compensate for changes in inlet oil concentration $C_i$ or the droplet size distribution [44, 45].

These issues could potentially be solved with reliable online OiW measurements. However, how to develop such a control solution is still an open question.

### 1.1.4 Oil-in-Water Monitoring

The available OiW monitoring technology utilizes different methods to estimate the OiW concentration, where every method exploits a meaningful difference between the oil and the water. In other words, the monitor must be sensitive to the oil while being insensitive to the water. This section addresses crude oil composition and summarizes the OiW monitor types used in this work.

Crude oil consists of a mixture of hydrocarbons and heteroatom compounds containing other atoms besides hydrogen and carbon, such as nitrogen, sulphur, and [46, 47]. When measuring oil concentration, typically only the hydrocarbons are measured. Total petroleum hydrocarbons can be classified by different structures and molecular formulas but are generally divided into three categories:

- Aliphatic: saturated hydrocarbons characterized by single C−C bonds
- Aliphatic: unsaturated hydrocarbons characterized by two C=C bonds or more C≡C.
- Aromatic: hydrocarbons characterized by ring structures.

The simplest aromatic hydrocarbon, benzene, has a configuration of six carbon atoms with the general molecular formula $C_6H_6$. Examples of aromatic hydrocarbons are benzene, toluene, ethylbenzene, and xylenes (BTEX). For reporting the discharge concentration, offline reference methods are used, such as the GC-FID method in the case of OSPAR. These methods typically use extraction chemicals and some compounds are lost in the process and thus not measured. The definition of oil in PW is, therefore, ambiguous as it depends on the type of reference method used to measure it. Since the measurement of OiW is highly method-dependent, results from different methods cannot be compared meaningfully [46]. As a consequence of the method dependency for measuring OiW, the total petroleum hydrocarbons are often classified as dispersed and dissolved hydrocarbons instead of saturated, unsaturated, and aromatics, as seen in Fig. 1.8.

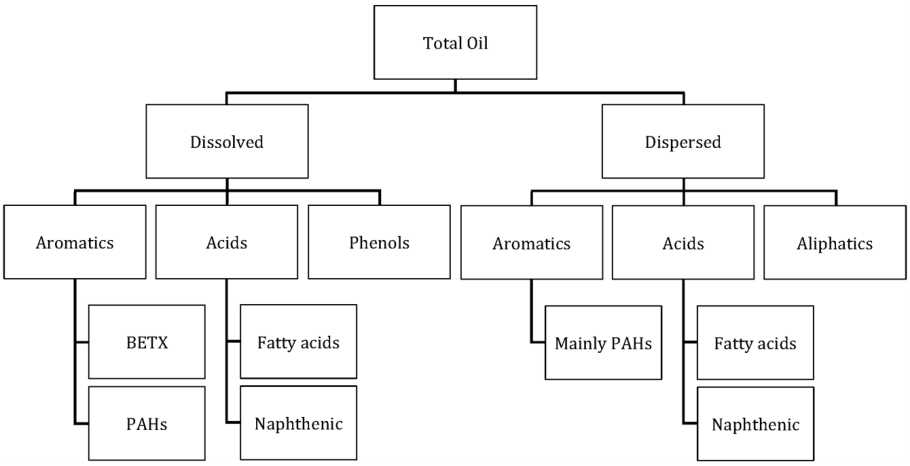


**Fig. 1.8:** An overview of crude oil composition [46].

The offline reference methods, like OSPAR, are typically measured in an onshore laboratory and are time-consuming processes. To compensate for this, online OiW monitors are increasingly used to measure the PW continuously for reporting [9, 46, 48]. In this thesis, ultraviolet (UV)-fluorescence-based monitors have been used to measure the OiW concentrations.

### UV-Fluorescence Monitors

The fluorescence-based monitor used in this thesis detects aromatic hydrocarbons in the OiW mixture [49]. As the PW mixture flows through the sample cell, the aromatic compounds absorb UV-light emitted from a fluorescent lamp. As the aromatic oil relaxes to its ground state, light at a longer wavelength is emitted, which is detected by a light sensor measuring the light

intensity. The light intensity is measured as a raw fluorescence unit (RFU), which is then transformed to concentration in parts per million (ppm) or mg/L through a calibration curve. It is important to point out that as the fluorescence-based monitor measures the aromatic content, it will measure both dispersed and dissolved oil, as seen in Fig. 1.8. An image of the OiW monitor is shown in Fig. 1.9.


**Fig. 1.9:** The TD4100-XDC UV-fluorescence Oil-in-Water (OiW) monitor by Tuner Designs.

## 1.2 Motivation for Control based on Online Oil-in-Water Monitors

As the volume of PW from oil and gas reservoirs increases, discharge legislation tends towards zero-discharge policies, and improved PWT is required. With the space and weight limitations on offshore installations and the high cost of pumping PW onshore for treatment, improvements in the systems separation efficiency are preferred. While the PW legislation is based on the measurement of OiW concentration and volume of PW, the offshore PWT systems do not utilize measurements of OiW concentration for control of the process. Instead, pressure measurements in the form of PDR are used to control the steady-state separation efficiency indirectly. However, the separation efficiency $\varepsilon_{oil}$ changes dynamically, as the PWT system is subjected to disturbances and PDR and $\varepsilon_{oil}$ are uncorrelated in some operating conditions. As PDR can only detect changes in flow rate, a PDR-based control system can only respond to and mitigate flow rate disturbances but cannot handle changes in inlet concentration or droplet size distribution [44, 45].

As online OiW monitors to measure the PW discharge are already mandatory for Danish oil and gas operators, it seems natural to use the measurements to control the discharge directly. By installing OiW monitors at the inlet and underflow of the hydrocyclone, the dynamic de-oiling efficiency could be measured and potentially controlled instead. With reliable OiW measurements, such a solution will likely improve the separation performance significantly and reduce the environmental impact of PW discharge.

### 1.2.1 Motivation for Hydrocyclone Modeling

Optimal controllers like MPC can be formulated to optimize the system performance. To develop such controllers, a reasonably precise and simple model is often needed.

Many studies have used computational fluid dynamics (CFD) modeling of hydrocyclones to optimize the hydrocyclone geometry and investigate the effect of different operating conditions on the separation efficiency [36,50–53]. Some CFD models have been validated experimentally [37,54], but although they can be accurate, the computational intensity makes them less suitable for control design.

Models that explain the underlying separation mechanism are generally preferred. Therefore, some research has focused on developing grey-box models of de-oiling hydrocyclones. A substantial amount of research has been done on droplet trajectory models, where often empirically determined expressions for the velocity fields inside the hydrocyclone are used to determine the trajectory of a given droplet size [55–57]. If the droplet size distribution and inlet concentration are known, the separation efficiency can be calculated. Such approaches have been extended with models describing the pressure-flow relationship in the hydrocyclone to calculate the fluid velocity fields needed for the droplet trajectory models [58,59]. As the pressure-flow relationship and the droplet trajectory analysis methods are generally static considerations, the separation dynamics are either based on the valve dynamics [59] or mass balances [58]. While such approaches have been seen to reasonably describe the steady-state separation efficiency, the dynamics remain invalidated. Therefore, there is an incentive to develop validated models of the OiW dynamics to support the design of OiW-based control.

## 1.3 Outline of the Papers

This thesis consists of an extended summary followed by papers A–E. The extended summary describes the background and motivation of the project and establishes the connection of the paper's contributions. An overview of

how the papers relate to each other is shown in Fig. 1.10. The remainder of this section describes the motivation of each of the paper's contributions.

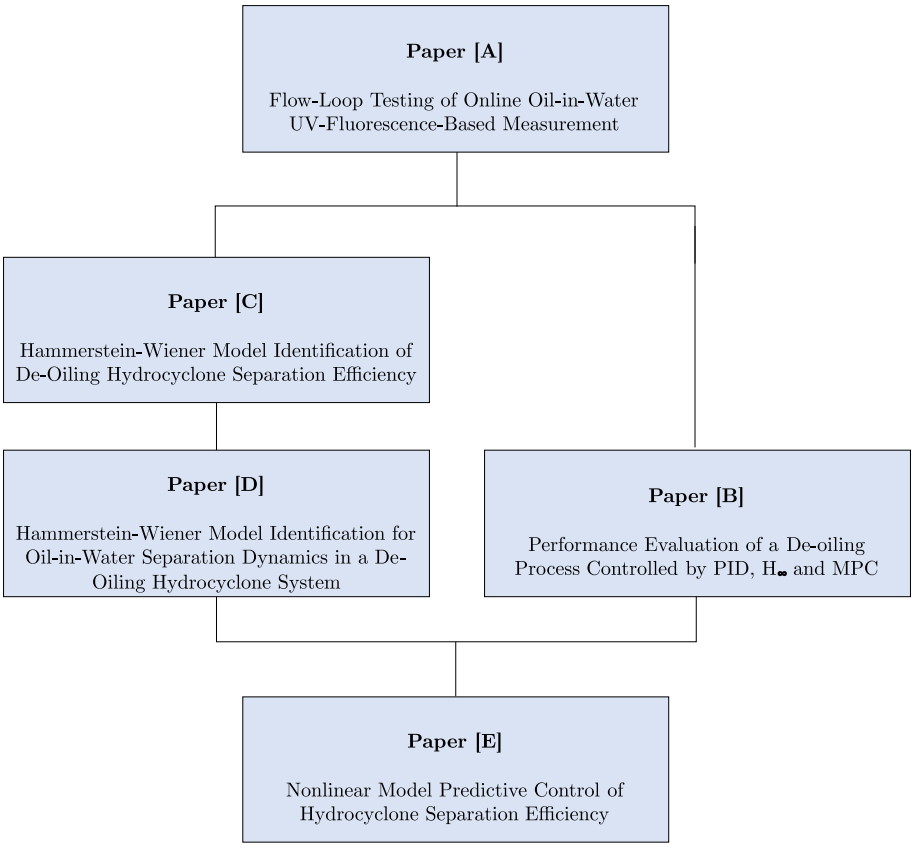


**Fig. 1.10:** Overview of the enclosed papers.

### 1.3.1 Motivation for Paper A

Although online OiW monitors are currently installed on offshore oil and gas facilities to support reporting of PW discharges and are sometimes used for process optimization, they are not directly used for control. To develop OiW-based control for offshore PWT processes, reliable measurements of the OiW content are crucial. As fluorescence-based OiW monitors are widely used for online measurement of OiW concentrations in offshore PW, paper A tests the effect of some process conditions on fluorescence-based OiW monitors. These experiments were used to gain confidence in the selected OiW monitors and make changes to the pilot plant to guarantee better conditions for the monitors.

### 1.3.2 Motivation for Paper B

There has been a lot of focus on improving the PDR-based control. Although PDR is correlated with the steady-state efficiency under some operating conditions, it is not a direct measure of the separation performance. Offshore PWT systems are often subject to varying production flow rates due to, e.g., slug flow [60]. Some advanced MIMO controllers have been designed to coordinate the control of the water level and PDR such that the effect of the flow variations on PDR is mitigated, such as a robust $H_\infty$ controller [40] and an MPC [41]. The performance of the $H_\infty$ controller was evaluated using OiW monitors by Durdvic et al. [61]. While MPC has the potential to perform better as it is based on optimization, an evaluation of the performance measured by OiW monitors was missing.

Paper A extends the performance evaluation by investigating other performance indices of the PID, the robust $H_\infty$, and the MPC. The results give insight into how separation performance can be defined, which is helpful in developing a control policy for OiW-based control. In addition, the PDR-based control solutions also serve as a baseline for new OiW-based control solutions where the same performance metrics can be used for evaluation.

### 1.3.3 Motivation for Paper C and D

In order to develop control solutions of the hydrocyclone's OiW dynamics, some reasonably precise and control-oriented models are needed. Although some grey-box approaches based on droplet-trajectory analysis have been seen to fit reasonably well to steady-state efficiency data, the dynamics have either not been validated or still need some improvement [15,58]. These models require measurements of the droplet size distribution, which complicates the model validation as well as the implementation. Interestingly, these models combine static nonlinearities and dynamics, which resemble a well-known family of block-oriented models. In paper C types of block-oriented models, known as Hammerstein-Wiener (HW) models, are identified from dynamic data collected at a testing facility. The identification experiment emulates an offshore PWT plant with active level and PDR control loops and installed OiW monitors subjected to varying production. The approach in paper C was extended in paper D to the discharge concentration and discharge rate, and the effect of using the inlet concentration as a model input is investigated. The proposed models proved capable of capturing most of the OiW dynamics.

### 1.3.4 Motivation for Paper E

While PDR-based control aims to indirectly control the steady-state efficiency of the de-oiling hydrocyclone, paper E uses an efficiency model obtained in paper C and paper D to develop a nonlinear model predictive control (NMPC) to optimize the dynamic separation efficiency. The developed NMPC solution is a cascaded control with the PDR controller in the inner loop. This way, the developed control solution builds on top of the already existing control solution. It is demonstrated through simulation that the developed solution can improve the separation efficiency significantly compared with the preexisting PID-type solution.

# Chapter 2

# Preparation for Online Oil-in-Water Monitoring

For the successful development of OiW-based control solutions, a reliable OiW measurement is crucial. Ideally, the OiW measurement should only be sensitive to the oil content in the PW. Therefore, the chosen UV-fluorescence monitors were tested during different conditions before further use. This chapter describes the testing facility, presents some results from testing fluorescence OiW monitors in paper A, and some upgrades to the testing facility to improve the OiW measurements.

## 2.1 Produced Water Treatment Testing Facility

The testing facility was initially constructed to investigate the effects of slugging [62] and potential advanced control solutions to reduce the adverse effects of slugging [63]. In recent years, the testing facility has been used to investigate different OiW monitor technologies [64], membrane filtration for PWT [65], hydrocyclone modeling [66] and OiW-based control in this work.

In summary, the configurations of the testing facility used in this work include the following:

- **A supply tank** located at the bottom of the facility with two mixers to obtain a homogenous emulsion of oil in water. A centrifugal pump is used to supply the mixture to other subsystems. The supply tank was used in all experiments on the facility to keep a constant mixture of water and oil. The oil used in all experiments is a non-detergent Midland Society of Automotive Engineers (SAE) 30 engine oil [67].
- **A pipeline riser subsystem** with 30m horizontal, 12m inclined, and 6m

vertical pipe to emulate slug flow conditions. Only the vertical pipe is used in the experiments to direct the OiW mixture into the three-phase separator tank. This subsystem includes a topside control valve, pressure transmitters, flowmeters, and a compressor with a supply pressure of 7 barg to inject air into the riser.

- **A separator tank subsystem** with a pressurized separator tank with control valves, level transmitters, flowmeters, and pressure transmitters. The separator tank has a diameter of 0.6 m and maximum operating pressure of 10 barg. The height of the installed weir plate is 0.3 m.
- **A hydrocyclone subsystem** consisting of a manifold with two industrial Vortoil hydrocyclones with the necessary control valves, flowmeters, and pressure transmitters. Only a single hydrocyclone liner was used in this work. At the inlet and underflow of the hydrocyclone, sampling ports are installed to connect the OiW monitors.
- **Four OiW monitors** installed on moveable platforms that can be connected to sampling ports in different locations on the testing facility.

The testing facility, with the three-phase separator tank, the two industrial hydrocyclones installed in cylindrical housings, and an OiW monitor mounted on a moveable platform, is shown in Fig. 2.1.

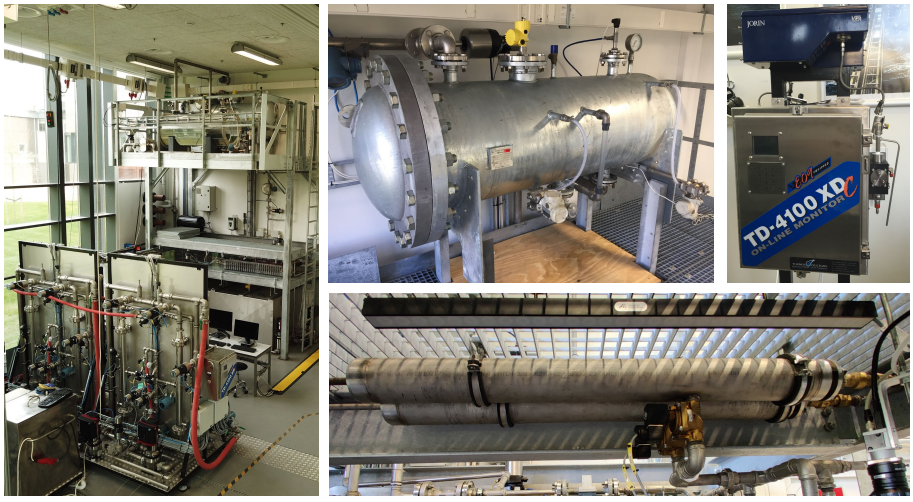


**Fig. 2.1:** Photos of the testing facility, the three-phase separator tank, the Turner TD-4100XDC UV-fluorescence OiW monitor mounted on a moveable platform, and the hydrocyclone liners.

## 2.2 Calibration and Challenges of UV-Fluorescence Monitors

For the UV-fluorescence monitor, a calibration curve must be established between the monitor's RFU and known oil concentrations. To establish this curve, multiple points are needed to discover potential nonlinear trends. The monitor manufacturer recommends using two (if the calibration curve is linear) or more points and applying ordinary least square (OLS) to fit the calibration curve to the data. In an offshore situation, samples taken from the process would be analyzed with a reference method such as GC-FID to obtain the known concentration values for the calibration. An example of a calibration curve obtained using OLS on the oil used in this study is shown in Fig. 2.2. The results clearly show a linear relationship between the RFU and the oil concentrations at these concentrations.

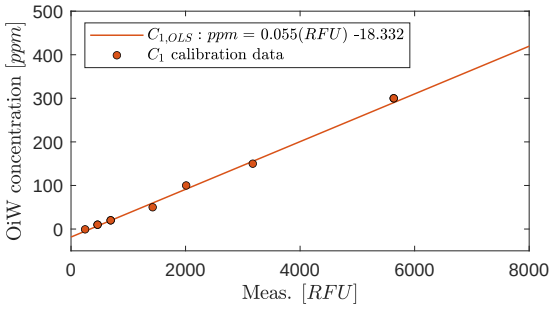


**Fig. 2.2:** An example of manufacturer-recommended calibration procedure using ordinary least squares (OLS).

In a joint publication by Hansen et al. [24], the OLS method was compared with a weighted least square (WLS) approach. Multiple solution standards were prepared by diluting a stock solution of iso-propanol alcohol and Midland non-detergent engine oil with tap water. The procedure of injecting samples and typing in the solution values is shown in Fig. 2.3. Ten samples were used at each of the concentrations (0,10,20,50,100,150,300) ppm for a total of 70 samples per calibration. Although the manufacturer-recommended procedure only uses a single sample per calibration standard, 70 points were used for the OLS calibration for fairness.

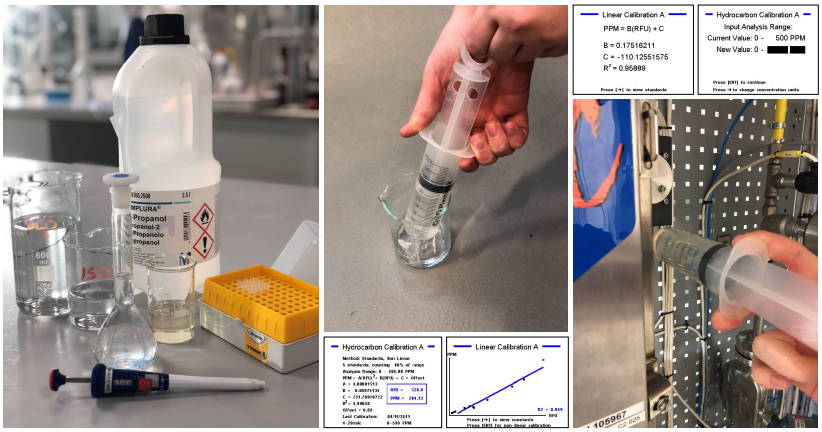


**Fig. 2.3:** Photos showing the preparation of calibration standards, the injection of samples into the monitor view cell, and the resulting calibration curve from the monitor display.

When using OLS, it is assumed that the calibration process has the same variance irrespective of the concentration, i.e., a homoscedastic process. The results in Fig. 2.4 show that this is not the case, as the variance is seen to be larger at higher concentrations. The uncertainty of the calibration process is heteroscedastic, and to take this into account, the inverse of the variance observed at each concentration is used as a weighting factor, which emphasizes the measurements with the smallest variance in the calibration curve as seen in Fig. 2.4.

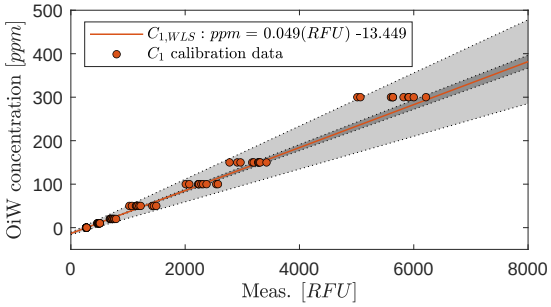


**Fig. 2.4:** Example of using weighted least squares (WLS) for obtaining the calibration curve. The inner dashed lines are the 95% confidence interval, and the outer dashed lines are the 95% prediction interval.

The issue with the recommended calibration method using only single points is that the variance can significantly affect the resulting calibration curve. An experiment by Hansen et al. [24] on a flow loop showed that the WLS calibration gave more reproducible results and results that were closer

to the target concentration of the mixture. Based on these observations, the OiW monitors were calibrated using the WLS method in all of the presented work.

### 2.2.1 UV-Fluorescence Monitor Challenges

A comprehensive overview of issues related to UV-fluorescence monitors is given in Hansen et al. [24]. As highlighted in section 1.1.4, the UV-fluorescence-based monitors are sensitive to the aromatic compounds in the PW. However, they are known to be influenced by other factors such as:

- Changes in the ratio of aromatic to aliphatic hydrocarbons [46].
- Inner filter effects, i.e., the attenuation of the excitation light by concentrated samples or the attenuation of the emitted light due to reabsorption by the sample [68, 69].
- Chemical quenchers, i.e., the presence of molecules that reduce the fluorescence intensity [69].
- Degradation of monitor components.
- Fouling of the view cell [49].

As a previous joined study by Bram et al. [15] suspected that the OiW monitors were flow-dependent, an investigation was carried out in paper A. Different scenarios were tested on the testing facility based on the configura-

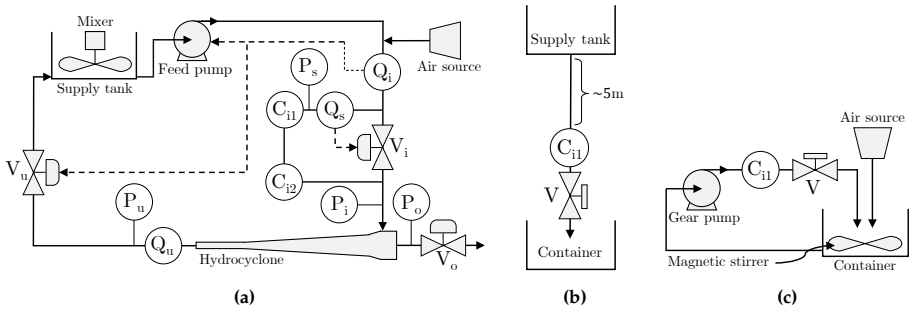


**Fig. 2.5: (a):** The system configuration for flow rate dependency tests, with a centrifugal pump to supply the oil/water mixture, flow meters to measure the flow in the main-stream $Q_i$ and the side-stream $Q_s$. The flow through the OiW monitors $C_{i1}$ and $C_{i2}$ is controlled by manipulating the control valve $V_i$ and the main-stream flow is either controlled with the underflow valve $V_u$ or the feed pump speed. **(b):** Setup used to test for the influence of air. **(c):** Gravity-fed setup for testing the flow rate dependency. All figures are modified from paper A.

tion presented in Fig. 2.5a, and some stand-alone tests were carried out with the setups in Fig. 2.5b and Fig. 2.5c, to test the effects of changing flow rate, and gas bubbles.

### Flow-dependency tests

To test the influence of variable flow, the OiW monitor was gravity-fed with tap water and demineralized water with two different opening degrees of the valve $V$ in Fig. 2.5b, corresponding to flow rates of 1.1 L/min and 1.7 L/min. The time series of successive repetitions of the experiment with demineralized water is seen on the upper plot in Fig. 2.6. The mean values of the time series seem to indicate a small difference between the two flow rates, and the grand mean of the RFU with the high flow (1.7 L/min) is 2% lower than the grand mean of the RFU with a low flow rate (1.1 L/min). This is only a small difference, and while the measurement was suspected to increase with increasing flow rate, the result is the opposite. With tap water, the difference between the grand means of the two flow rates was only 0.2%, indicating that the observations by Bram et al. [15] were caused by system effects.

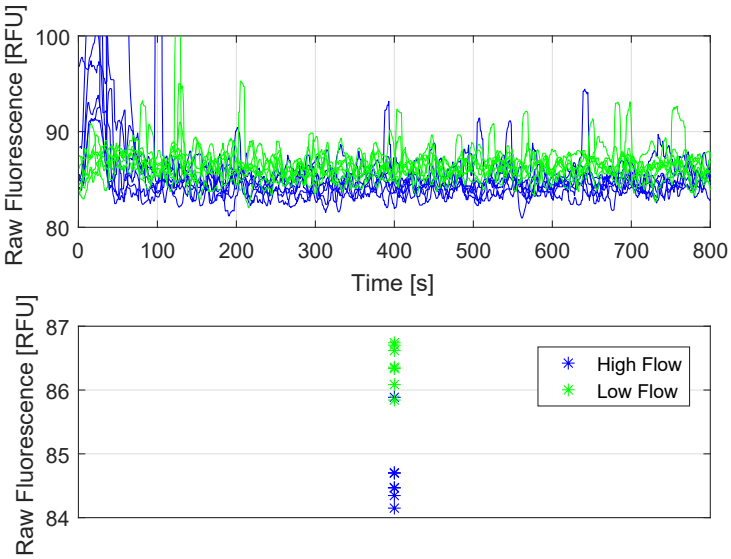


**Fig. 2.6:** Time series of raw fluorescence unit (RFU) from the gravity-driven tests with demineralized water (top) and the means of the time series data in the time period 200-800 s (bottom). *High flow* corresponds to a flow rate of 1.7 L/min and *low flow* corresponds to 1.1 L/min.

### Influence of gas bubbles on the OiW measurement

It was suspected that air bubbles could influence the monitor reading. To test this, a container with a magnetic stirrer was filled with tap water and circulated through one of the OiW monitors, as illustrated in Fig. 2.5c. Tap

water was used as the only liquid as it was found to fluoresce and avoid any effects related to the mixing of oil. The gear pump was set to a constant speed, and the manual valve $V$ was adjusted to reach a constant flow rate of $\approx 1.1$ L/min. The system was left running until the RFU measurement had reached a steady state. Gas bubbles were introduced by mixing air into the container with an air source. The results are seen in Fig. 2.7, where the OiW measurement represented by the RFU is steady with a mean value of 1665 RFU during the initial 600s. The introduction of air in the period of 600-1200 s results in an increase of 118 RFU, corresponding to an increase of about 7%, clearly indicating that air increased the OiW concentration measurement.

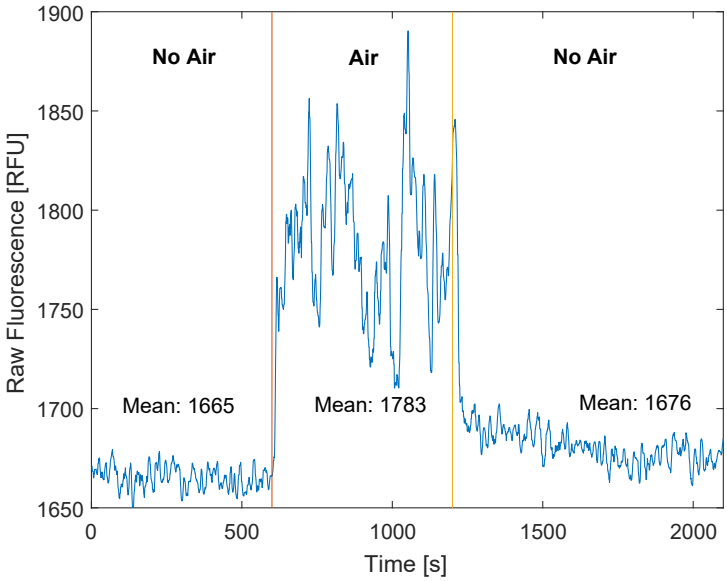


**Fig. 2.7:** The raw fluorescence unit (RFU) measured by the monitor. Air bubbles are introduced in the time period 600-1200 s. The figure is from paper A.

### 2.2.2 Testing Facility Related Challenges

Paper A highlights some system-related effects that can affect the OiW measurements. Some potential effects are:

- Oil accumulating or being freed from surfaces and/or dead volumes.
- Varying shearing causing changing droplet size distribution.
- Introduction of air bubbles when mixing oil and water.

- Contamination and microbiological growth.
- Potential unrepresentative sampling due to the use of T-junctions as sampling probes and the lack of iso-kinetic sampling.
- Long distance between sampling points and OiW monitors introducing a delay.
- Stratification of oil due to low flow velocity (laminar flow).

To recreate the observed variation in OiW concentration during variable flow rates, the mainstream flow rate was controlled and varied between 6 L/min, 24 L/min, and 30 L/min by varying the speed of the feed pump, which resulted in increased RFU values of 55% and 83% for the two OiW monitors, respectively as seen in Fig. 2.8. Keeping the pump speed fixed and varying the flow rate by controlling $V_i$ reduced the increase to 26% and 24%, indicating that both the total flow rate and the pump speed had an influence.

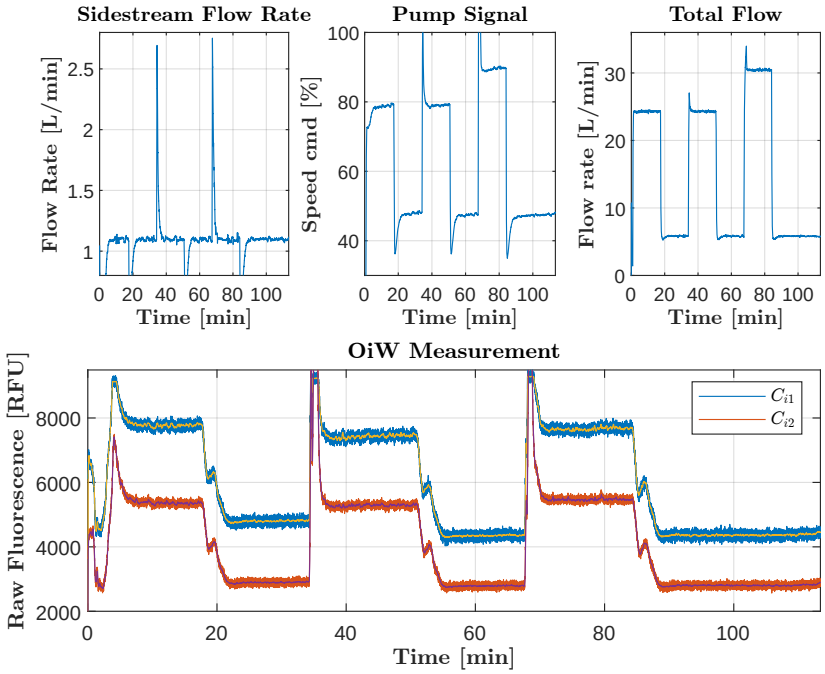


**Fig. 2.8:** Variations in the total flow rate $Q_i$ introduced with the pump, while the flow rate $Q_s$ through the OiW monitor is controlled at 1.1 L/min.

Variations in sidestream flow rate with constant pump speed and mainstream flow rate did not seem to affect the OiW measurement, which underlines that the variations seen are system effects. The effect did, however, seem to saturate at a flow of around 24 L/min and pump speed of 80-90%.

## 2.3 Oil-in-Water Monitor Sidestream Upgrade

The sidestreams were modified to remedy some of the observed systems and monitor related issues. Fig. 2.9 shows the installed OiW monitors after the modifications. The modification includes:


**Fig. 2.9:** Photos after installing four OiW monitors with two monitors on each sidestream. The sampling probes are installed in a vertical pipe section with flowmeters and control valves to maintain a constant flow rate through the monitors.

- Installation of the monitors closer to the sampling point to reduce the fluid travel length.
- Installation of two monitors in series for measurement redundancy.
- Installation of vertical pipe sections where the sampling probes are installed to reduce stratification at the sampling point.
- Installation of flow meters and control valves to maintain the sidestream flow rate within the recommended flow range.

A simplified P&ID diagram of the system after the modifications is shown in Fig. 2.10, with the OiW monitors installed on the inlet and underflow sidestreams. Flow controllers $FC_{is}$ and $FC_{us}$ are used to control the sidestream flow rates within the range recommended by the manufacturer using the installed flowmeters ($Q_{is}$ and $Q_{us}$) and control valves ($V_{is}$ and $V_{us}$). Additionally, the diagram shows the production flow controller $FC_{in}$ used to generate varying production flow in the experiments, the separator pressure controller $PC$, the level controller $LC$, and the PDR controller $PDRC$.

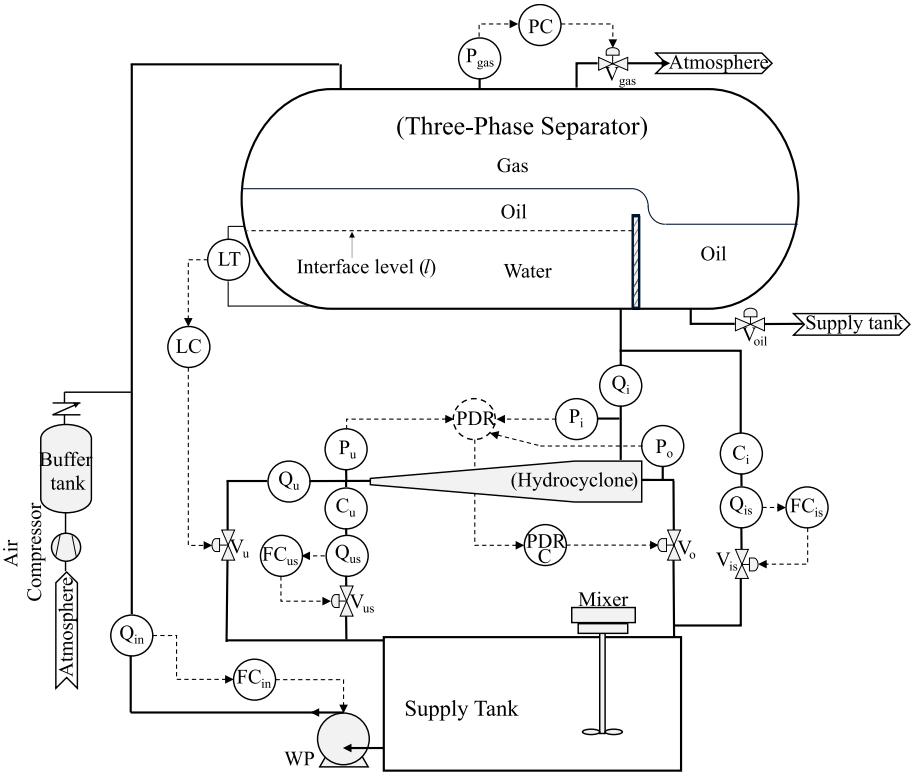


**Fig. 2.10:** Schematic of the testing facility with control loops and OiW monitors ($C_i$ and $C_u$) installed in sidestreams at the inlet and the underflow of the hydrocyclone. Specifications of actuators and sensors can be found in Table 2.1. The figure is modified from paper D.

Descriptions of the instrumentation corresponding to the symbols in Fig. 2.10 are listed in Table 2.1.

**Table 2.1:** Specifications of actuators and sensors.

| Symbol | Description | Type | Unit |
|---|---|---|---|
| $P_{sep}$ | Separator pressure | Siemens Sitrans P200 | bar |
| $P_i$ | Hydrocyclone inlet pressure | | |
| $P_u$ | Hydrocyclone underflow pressure | | |
| $P_o$ | Hydrocyclone overflow pressure | | |
| $Q_{in}$ | Separator inlet flow rate | Rosemount 8732 Electromagnetic flow meter | kg/s |
| $Q_i$ | Hydrocyclone inlet flow rate | Bailey Fischer Porter 10DX4311C Electromagnetic flow meter | L/s |
| $Q_u$ | Hydrocyclone underflow flow rate | | |
| $Q_o$ | Hydrocyclone overflow flow rate | Micro-Motion Coriolis Elite (CMFS010) Coriolis flow meter | kg/s |
| $Q_{is}$ | Inlet sidestream flow rate | Micro-Motion Coriolis Elite (CMFS010) Coriolis flow meter | kg/s |
| $Q_{us}$ | Underflow sidestream flow rate | Rosemount 8711 Electromagnetic flow meter | L/s |
| $V_{gas}$ | Separator gas valve | Bürkert 2875 + 8605 | – |
| $V_{oil}$ | Separator oil valve | Bürkert 8802-GD-I pneumatic valve systems | – |
| $V_i$ | Hydrocyclone inlet valve | | – |
| $V_u$ | Hydrocyclone underflow valve | | – |
| $V_o$ | Hydrocyclone overflow valve | | – |
| $V_{is}$ | Inlet sidestream valve | | – |
| $V_{us}$ | Underflow sidestream valve | | – |
| $C_i$ | Inlet sidestream OiW concentration | Turner Design TD-4100XDC fluorescence-based OiW monitors | ppm |
| $C_u$ | Underflow sidestream OiW concentration | | |
| $WP$ | Water pump | Grundfos CRNE 5-9 centrifugal pump | – |
| *Mixers* | Supply tank stirrers | Milton Roy Mixing HELISEM VRP3051S90 | – |

## 2.4 Conclusion

To gain confidence in the OiW monitor before deploying it for online OiW measurements, the effect of flow variations and gas bubbles on the OiW measurement with two (Turner TD4100-XDC) UV-fluorescence monitors was investigated. The results indicate that the monitors are insensitive to changes in flow rate within their recommended range of 1-2 L/min. The test with air bubbles resulted in an increased reading of about 7%, but further investigation is needed to quantify the effect of gas bubbles on the measurement. Variations in the OiW measurement were seen to occur with changes in pump speed and total flow rate. However, further investigation is needed to determine the underlying cause for these effects. To reduce some of these effects, some improvements were made to the sidestream sampling mechanism. The effect of varying concentration with pump speed and flow rate was also not observed when using the three-phase separator in papers B, C, and D.

# Chapter 3

# Performance Evaluation of Pressure Drop Ratio Control Using Oil-in-Water Monitors

PDR-based control has been widely used to control de-oiling hydrocyclones in the PWT systems due to the lack of reliable OiW monitor technology in the past. With new emerging technology and increased trust in online OiW measurements, control based on online OiW measurements could become a reality and potentially reduce the pollution of oil discharges from PWT facilities as concluded in chapter 2 which focused on preparing and applying OiW monitors.

Before using the OiW monitors as a feedback signal, it is valuable to use them to evaluate the performance of the PDR-based control to identify potential advantages and disadvantages of the PDR-based methods and different control methods in general. This way, OiW monitors can support the decision of a control policy for new advanced controllers to optimize the existing control solution. This chapter presents three PDR-based control solutions that were designed to mitigate the effects of changing production flow on the PDR and thus potentially also the separation efficiency as illustrated in Fig. 1.5 and Fig. 1.6. A presentation of the controllers and the underlying models is given, followed by the comparison results.

## 3.1 Models of Separator Level and Hydrocyclone Pressure Drop Ratio

In this section, the models of the separator level and the hydrocyclone PDR are presented, which were the basis for the design of the controllers presented in this chapter.

To model the water level, the mass balance for the separator is defined as

$$\frac{dV(t)}{dt} = Q_{in} - Q_{out}, \tag{3.1}$$

where $Q_{in}$ is the volumetric flow rate (the production flow) into the separator tank, and $Q_{out}$ is the volumetric flow rate leaving the separator tank. $Q_{out}$ is defined by the orifice equation

$$Q_{out} = C_v f(V_u)\sqrt{\frac{\Delta P}{\rho g}}, \tag{3.2}$$

where $\Delta P$ is the pressure drop over the underflow valve, $\rho$ is the density of water, $g$ is the gravitational acceleration, and $C_v$ is the valve orifice coefficient, which can be identified using experimental data. $f(V_u)$ is the valve characteristic curve explaining the relation between the valve opening degree $V_u$ and the area of the valve opening.

The liquid volume in the separator tank is a function of the varying water level $l(t)$. Inserting (3.2) in (3.1) and applying the chain rule gives

$$\frac{dV(t)}{dt} = \frac{dV(l(t))}{dl(t)}\frac{dl(t)}{dt} = Q_{in} - C_v f(V_u)\sqrt{\frac{\Delta P}{\rho g}}. \tag{3.3}$$

Isolating for the rate of change of the water level yields

$$\frac{dl(t)}{dt} = \frac{1}{\frac{dV(l(t))}{dl(t)}}\left(Q_{in} - C_v f(V_u)\sqrt{\frac{\Delta P}{\rho g}}\right). \tag{3.4}$$

The volume of the cylindrical water compartment $V(l(t))$ is given by the product of the area of a circular segment $A(l(t))$ and the length of the water compartment $L$

$$V(l(t)) = A(l(t))L = \left(r^2 cos^{-1}(\frac{r-l(t)}{r}) - (r-l(t))\sqrt{2rl(t) - l(t)^2}\right)L, \tag{3.5}$$

where $r$ is the radius of the separator.

The nonlinear model of the level was linearized around $l = 0.15$ m, with $V_u = 0.4168$ and $V_o = 0.1657$ and combined with a black-box model of

PDR [40]. The model consists of two second-order transfer function (TF) describing the input-output relationship from $V_o$ to PDR and from $V_u$ to PDR. The resulting state-space model is

$$\begin{bmatrix} \dot{l} \\ \ddot{x}_{V_u} \\ \dot{x}_{V_u} \\ \ddot{x}_{V_o} \\ \dot{x}_{V_o} \end{bmatrix} = \begin{bmatrix} -1.23e^{-5} & 0 & 0 & 0 & 0 \\ 0 & -0.9745 & -0.7606 & 0 & 0 \\ 0 & 1 & 0 & 0 & 0 \\ 0 & 0 & 0 & -0.9316 & -0.6540 \\ 0 & 0 & 0 & 1 & 0 \end{bmatrix} \begin{bmatrix} l \\ \dot{x}_{V_u} \\ x_{V_u} \\ \dot{x}_{V_o} \\ x_{V_o} \end{bmatrix} ... + \begin{bmatrix} -1.369e^{-3} & 0 & 1.7e^{-3} \\ -1 & 0 & 0 \\ 0 & 0 & 0 \\ 0 & 1 & 0 \\ 0 & 0 & 0 \end{bmatrix} \begin{bmatrix} V_u \\ V_o \\ Q_{in} \end{bmatrix} \tag{3.6}$$

$$\begin{bmatrix} l \\ PDR \end{bmatrix} = \begin{bmatrix} 1 & 0 & 0 & 0 & 0 \\ 0 & 0 & 2.7204 & 0 & 1.6872 \end{bmatrix} \begin{bmatrix} l \\ \dot{x}_{V_u} \\ x_{V_u} \\ \dot{x}_{V_o} \\ x_{V_o} \end{bmatrix} \tag{3.7}$$

## 3.2 Pressure Drop Ratio Control Solutions

In this section, the three control solutions for combined control of the water level in the three-phase separator tank and the hydrocyclone PDR are briefly presented. Two PID controllers that mimic the industrial solution are used as the benchmark for two advanced controllers. These two control solutions, $H_\infty$ and MPC, were evaluated based on previous investigations by Durdevic et al. [40] and Hansen et al. [41]. The three control solutions are designed as follows:

- **The PID control solution** evaluated in paper B was presented for the first time by Durdevic et al. [40] to mimic data from an offshore installation subjected to variable production. The level and PDR controllers are given by

$$\frac{U_{V_u}(s)}{E_l(s)} = -58.37 - \frac{1.067}{s} \tag{3.8}$$

  and

$$\frac{U_{V_o}(s)}{E_{PDR}(s)} = 0.1 + \frac{0.1}{s}. \tag{3.9}$$

- **The robust controller** in paper B is a suboptimal $H_\infty$ controller. To obtain such a controller, the linear fractional transformation (LFT) of the

closed-loop system is used, as illustrated in Fig. 3.1. The generalized system $P$ in Fig. 3.1 is given by the state space representation

$$\dot{x}(t) = Ax(t) + B_1 w(t) + B_2 u(t) \tag{3.10}$$
$$z(t) = C_1 x(t) + D_{11} w(t) + D_{12} u(t) \tag{3.11}$$
$$y(t) = C_2 x(t) + D_{21} w(t) + D_{22} u(t), \tag{3.12}$$

where $x(t)$ is the system state, $w(t)$ is the exogenous inputs, i.e., disturbances and reference signals, $z(t)$ is performance output, and $y(t)$ is the measurements. For the system considered, these signals are

$$w(t) = \begin{bmatrix} r_l \\ r_{PDR} \\ d \end{bmatrix}, u(t) = \begin{bmatrix} V_u \\ V_o \end{bmatrix}, z(t) = \begin{bmatrix} e_l \\ e_{PDR} \end{bmatrix}, y(t) = \begin{bmatrix} l \\ PDR \end{bmatrix}. \tag{3.13}$$

The aim of the $H_\infty$ design is to find a stabilizing controller $K$ which minimizes the $H_\infty$ norm of the lower LFT in Fig. 3.1, i.e., the transfer matrix from $w(t)$ to the performance output $z$ [70]. In the suboptimal case the requirement of the $H_\infty$ norm is relaxed to be less than a positive number $\gamma$

$$\|\mathcal{F}_l\|_\infty < \gamma. \tag{3.14}$$

Following this method, the controller can be designed to guarantee that the effect of the flow disturbance $Q_{in}$ on the separator water level and PDR is bounded. The controller $K$ is found as the solution of two Ricatti equations.

More about the $H_\infty$ control design is described by Durdevic et al. [40].

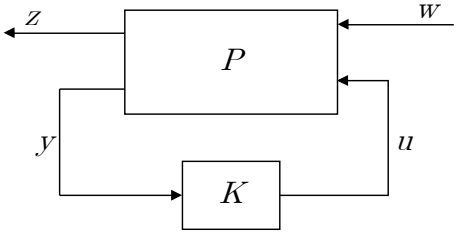


**Fig. 3.1:** General linear fractional transformation (LFT) representation of the closed-loop system.

- **The MPC controller** used in this work was first presented by Hansen et al. [41]. Similar to the design of the $H_\infty$ controller, the aim is to relax the control of the level to reduce variations in PDR. The MPC has the advantage that the upper and lower safety limits of the level can be specified directly as constraints in the formulation of the controller. The

PDR model in (3.6) and (3.7) was extended to include the rate of change of PDR and extended with a Hammerstein function to make the model valid in a broader range

$$V_{o,h} = \arctan(V_o k_1) k_2, \tag{3.15}$$

with $k_1 = 6$ and $k_2 = 0.2118$.

The MPC minimizes the following cost function by selecting the future control moves $\Delta\hat{u}(k+i|k)$ from the last input $u(k-1)$, based on measurements up to time $k$

$$J(k) = \sum_{i=1}^{H_p} \|\hat{y}(k+i|k) - r(k+i|k)\|^2_{Q(i)} + \sum_{i=0}^{H_u-1} \|\Delta\hat{u}(k+i|k)\|^2_{R(i)}. \tag{3.16}$$

In (3.16), $\hat{y}(k+i|k)$ is the predicted outputs of level and PDR based on the information at the $k$th timestep and $r(k+i|k)$ is the reference. The prediction horizon $H_p$ specifies the number of time steps the controller predicts ahead, and the control horizon $H_u$ is the number of steps with control moves. $Q$ and $R$ are weighting matrices, specifying the importance of reference tracking for the level and PDR and the actuation of $V_o$ and $V_u$. The essence of the design is to assign larger weights to the PDR and rate of change of PDR rather than to the level $l$, as well as to assign large weights to $V_u$. This effectively prioritizes tracking of PDR and suppresses moves of $V_u$ to minimize variations in $Q_{in}$.

Additionally, the water level is constrained as $0.1 \leq (l + 0.15) \leq 0.2$ to keep the level within the safety limits, and $V_u$ and $V_o$ are constrained due to their physical limitation and to keep them from fully closing. After finding the optimal trajectory of control moves, the first element is applied to the system, i.e., by setting $u(k) = u(k-1) + \Delta\hat{u}(k|k)$ and the optimization problem is repeated in the next time step. To remove the effect on the Hammerstein nonlinearity, the control output $V_{o,h}$ goes through the inverse Hammerstein function

$$V_o = \frac{\tan(\frac{V_{o,h}}{k2})}{k_1}. \tag{3.17}$$

## 3.3 Performance Evaluation of Pressure Drop Ratio Control

The experiments with varying production flow rates to compare the three control solutions were executed on the testing facility with the installed OiW

monitors, which are shown in Fig. 2.10 in chapter 2. To measure the performance of the separation system with the different controllers, two OiW monitors were used, one to measure the inlet oil concentration $C_i$ and one to measure the discharge concentration $C_u$. The OiW monitors were calibrated using the WLS method as described in section 2.2. The experiment uses the following controllers and conditions, as illustrated in Fig. 2.10:

- The oil and water mixture is continually mixed in the supply tank.
- Variations in production flow rate $Q_{in}$ into the separator are created by controlling the speed of the feed pump with the flow controller $FC_{in}$.
- The separator pressure $P_{gas}$ is controlled by a PID controller $PC$ with control valve $V_{gas}$ as actuator and a target of 7 bara.
- Air is supplied by the compressor and buffer tank at a pressure of 8 bara.
- The sidestream flow rates $Q_{is}$ and $Q_{us}$ through the OiW monitors are controlled by PID controllers $FC_{is}$ and $FC_{us}$, that actuates the control valves $V_{is}$ and $V_{us}$. The setpoint is 1.5 L/min.
- The separator level is controlled by one of the three controllers PID, $H_\infty$ and MPC (denoted $LC$). The setpoint is 0.15m.
- The PDR is controlled by one of the three controllers PID, $H_\infty$ and MPC (denoted $PDRC$). The setpoint is 2.

Different measures of performance were used for the comparison of the three controllers. The discharge concentration $C_u$ is a natural candidate to measure performance because of the discharge legislation. The separation efficiencies $\varepsilon_{oil}$ and $\varepsilon_{red}$ defined in (1.3) and (1.4) are also natural choices as they are a measure of separation performance by definition. Additionally, the volumetric rate of oil discharge, i.e., the product of discharge concentration $C_u$ and flow $Q_u$, was also examined as it directly measures the discharge, i.e.,

$$Q_{u,oil} = C_u Q_u. \tag{3.18}$$

Only a very small difference was observed between the oil removal efficiency $\varepsilon_{\text{oil}}$ in (1.3) and the concentration-reducing efficiency $\varepsilon_{\text{red}}$ in (1.4). Thus, results are therefore presented using $\varepsilon_{\text{red}}$ in the following.

The PID level controller actuated the underflow valve aggressively to keep the level close to the reference value, as seen in Fig. 3.2. This directly impacted the PDR value, which made the PDR controller actuate $V_o$ aggressively.

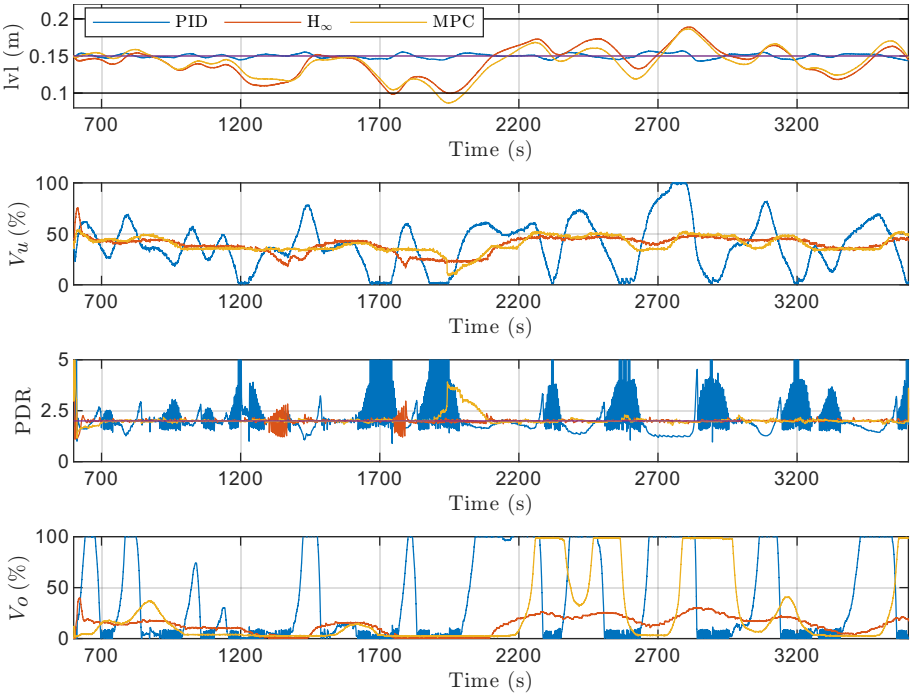


**Fig. 3.2:** Comparison of the water level with indicated alarm limits (black horizontal lines), valve opening degrees of $V_u$ and $V_o$, and the PDR. The figure is modified from paper B.

The PID controllers saturated $V_u$ and $V_o$ fully open and closed for extended periods. Large opening degrees of $V_u$ corresponded to decreased flow split, which is also evident in the PDR in Fig. 3.2. The underflow valve $V_u$ effectively chokes $V_o$ when it opens more than approximately 50%. The aggressive actuation of $V_u$ and the resulting variations in flow split cause variations in the separation performance, as seen in Fig. 3.3. When the PID controller opened $V_u$ beyond the critical value, the efficiency was reduced significantly due to the low flow split. Similarly, when $V_u$ is closed, the vortex in the hydrocyclone cannot be sustained, and the efficiency is thereby reduced.

Both the MPC and the $H_\infty$ controller successfully relaxed the level control, which reduced the variations in the actuation of $V_u$ and resulted in a steady inlet flow rate $Q_i$ to the hydrocyclone. This reduced the variations in separation efficiency $\varepsilon_{\text{red}}$ and discharge concentration $C_u$ as well as the discharge rate $Q_{u,oil}$, as seen in Fig. 3.3.

It can be challenging to compare the performance of the controllers directly based on the efficiency, OiW discharge concentration, or oil discharge rate, as the controllers can perform better in some periods and worse in others.

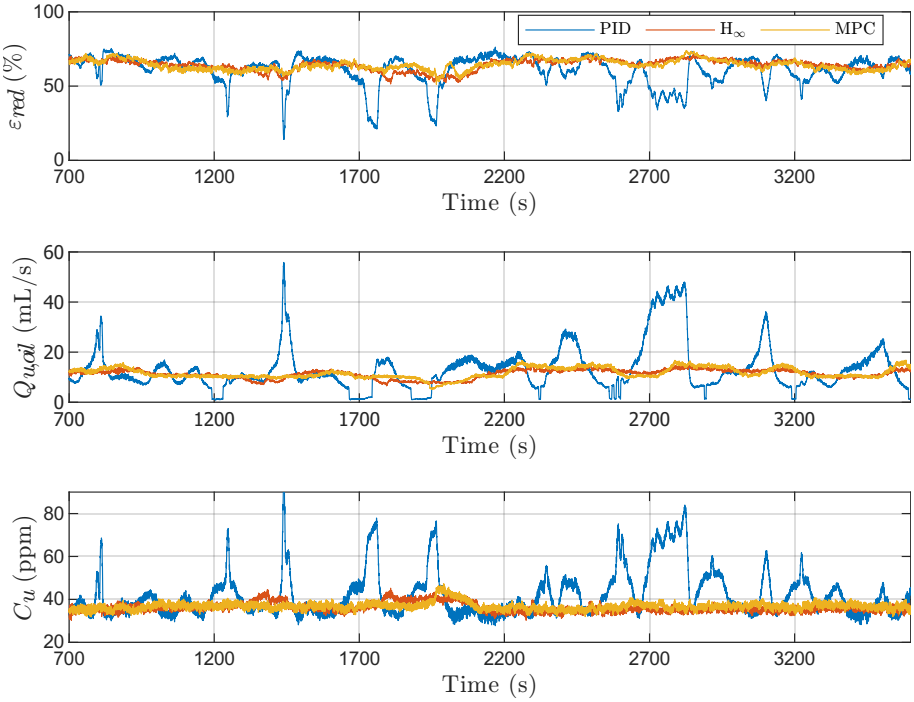


**Fig. 3.3:** Comparison of the three control systems with separation efficiency $\epsilon_{red}$, discharge rate $Q_{u,oil}$, and discharge concentration $C_u$.

Therefore, some accumulated values were compared in paper B. Some of these numbers are presented in Table 3.1, such as the total volume of oil entering the hydrocyclone (Inlet oil volume) and the total volume of oil discharged (Underflow oil volume). Although the goal of the PWT process is to reduce the discharge of oil, the increased performance should ideally

**Table 3.1:** Total volumes of liquid entering and exiting the hydrocyclone throughout the experiments.

| Total accumulated | Unit | PID | $H_\infty$ | MPC |
|---|---|---|---|---|
| Inlet liquid volume | L | 1018.73 | 1031.89 | 1033.70 |
| Inlet oil volume | mL | 112.85 | 107.98 | 109.48 |
| Overflow oil volume | mL | 71.64 | 70.85 | 72.57 |
| Underflow oil volume | mL | 41.21 | 37.13 | 36.91 |
| Overflow water volume | L | 61.86 | 74.24 | 73.99 |

not reduce the production of oil. The MPC processed the largest volume of PW with a total of 1033.7 L and simultaneously separated the most oil (72.57 mL), and discharged the lowest total volume of oil (36.91 mL). The largest volume of oil (112.85 mL) entered the hydrocyclone with the PID control due to the periods of large $Q_i$ caused by the aggressive level controller. The PID controller also achieved the lowest volume of water in the overflow, but this is also due to the periods of large $Q_i$, which choked the overflow valve, effectively reducing the flow split even when $V_o$ is fully open.

Both the $H_\infty$ and MPC failed to keep the level within the level constraints at one instant during the experiment, as seen in Fig. 3.2. This is a consequence of the side-stream configuration, which continuously passes 1.5 L/min through the OiW monitors. The sidestream flow is rejected back into the mixing tank, which was not considered in the separator level model. This flow corresponds to 6.25% of the mean production flow rate $Q_{in}$ in the experiment. However, this is a limitation of the testing facility, which would not be observed on an offshore platform as the sidestream flow rate is insignificant compared with the total production.

One interesting observation is that the hydrocyclone can have periods of high efficiency and low discharge concentration but simultaneously have a high oil discharge rate. This is seen in Fig. 3.3 around $t = 2100$ s where the PID achieved higher separation efficiency and lower discharge concentration than the $H_\infty$ and MPC but a significantly higher discharge rate. This occurs because the separation efficiency increases with increasing $Q_i$ (effectively $Q_u$) over some range, and the discharge rate depends on $Q_u$. Additionally, the inlet concentration increased with $Q_i$ in some periods, which may further increase separation efficiency and the discharge rate. This may be explained by the reduction of residence time in the separator tank at higher flow rates, thus reducing the separation efficiency of the separator tank according to (1.1).

While separation efficiency is intuitive, per definition, it only explains the performance of the hydrocyclone itself. Therefore, a MIMO controller that maximizes the separation efficiency of the hydrocyclone alone may lead to reduced separation efficiency of the separator tank and, thus, possibly reduced combined separation efficiency. Therefore, such a controller needs to consider the combined system efficiency. Similarly, the lowest discharge concentration does not guarantee the least total oil discharge. The discharge rate differs from efficiency and discharge concentration by taking both concentration and flow into consideration. Therefore, the discharge rate measures the de-oiling performance of the combined system.

## 3.4 Conclusion

The comparison of the three control solutions PID, $H_\infty$ and MPC showed that the MPC and $H_\infty$ significantly reduced the disturbance effect of $Q_{in}$ on PDR by relaxing the level control. This transferred into a steadier $Q_i$ and PDR and effectively reduced variation in separation efficiency, discharge concentration, and discharge rate. Overall, the MPC achieved the lowest total discharge of oil and performed better on most of the performance measures. The performance of the $H_\infty$ was within reach of the MPC as both controllers mitigate the effect of the fluctuations in the production flow. The observations from the comparison can be summarized as:

- Reducing variations in $Q_i$ and PDR transfers into reduced variation in separation performance measured as separation efficiency $\varepsilon_{red}$, discharge concentration $C_u$, and discharge rate $Q_{u,oil}$.
- PDR does not correlate with the separation efficiency under all operating conditions.
- The separation efficiency increases with the inlet flow rate until a critical value beyond which the efficiency deteriorates.
- The hydrocyclone inlet OiW concentration $C_i$ is correlated with the inlet flow rate $Q_i$.
- Some periods with high separation efficiency and low discharge concentration coincide with periods of larger discharge rate due to the increased discharge flow rate.

In conclusion, the results indicate that the MIMO controllers achieved successful disturbance rejection of $Q_{in}$, resulting in an improved and steadier separation performance. However, the PDR is not always correlated with the separation performance indices $C_u$, $Q_{u,oil}$, and $\varepsilon$, which motivates the development of OiW-based control. The separation performance clearly depends nonlinearly on $V_u$, $V_o$ and seems to also depend on $C_i$ under some conditions.

# Chapter 4

# Modeling of Oil-in-Water Separation Dynamics

To design OiW-based controllers, a dynamic model of the input-output behavior of the de-oiling hydrocyclone is required. In chapter 3, the separation efficiency $\varepsilon_{red}$, discharge concentration $C_u$, and discharge rate $Q_{u,oil}$ were used to evaluate the performance of PDR-based controllers. Therefore, these performance indices are potential controlled variables in the OiW-based control design. A nonlinear relationship was noticed between the control valve opening degrees $V_u$, $V_o$, and the separation performance. In paper C and D, a nonlinear block-oriented model known as the Hammerstein-Wiener (HW) model was used to model the OiW dynamics.

The general HW model consists of a linear dynamic block sandwiched between two nonlinear static function blocks, as seen in Fig. 4.1. The HW model simplifies to a Hammerstein model if the output nonlinearity is missing, while a linear dynamic system followed by a nonlinear static function is a Wiener model. Hammerstein, Wiener, and HW models have been widely used for their relative simplicity and capability to describe many nonlinear dynamic systems [41, 71–73].

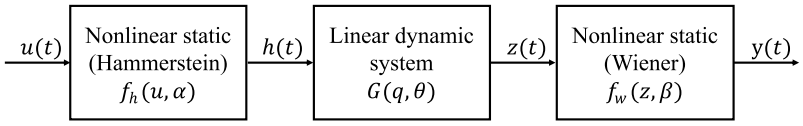


**Fig. 4.1:** General Hammerstein–Wiener (HW) model structure. The figure is from paper D.

In this chapter, a methodology is presented to identify HW models of the OiW separation dynamics. The identification experiment was identical to the PID scenario studied in chapter 3, but $V_o$ was adjusted to only use half of its

valve travel to reduce its effective size and improve the resolution of $V_o$. Thus the identification experiment mimics an offshore PWT facility with installed OiW monitors at the inlet and underflow of the hydrocyclone, subjected to variable production flow rates. Such a scenario may be realistic with the legislative incentive to install OiW monitors.

## 4.1 Hammerstein–Wiener Nonlinear Model Structure and Identification Approach

A generalized version of the proposed HW model in paper C and D can be written as follows

$$h(t) = f_h(u(t), \alpha) \tag{4.1}$$
$$z(t) = G(q, \theta)h(t) \tag{4.2}$$
$$y(t) = f_w(z(t), \beta) + e(t) \tag{4.3}$$

where $u(t) \in \mathbb{R}^{n_u}$ is the input, $y(t) \in \mathbb{R}^{n_y}$ is the output, $e(t)$ denotes the measurement noise/output error, and $t$ denotes the sampling instances $t = 0, 1, 2, \cdots, N$. The vector functions $f_h(\cdot, \alpha)$ and $f_w(\cdot, \beta)$ are the Hammerstein and Wiener static nonlinear functions, respectively, with parameter vectors $\alpha \in \mathbb{R}^{n_h}$ and $\beta \in \mathbb{R}^{n_w}$. The linear time-invariant dynamic model $G(q, \theta)$ is a TF matrix of dimension $n_y \times n_u$ and parameter vector $\theta \in \mathbb{R}^{n_\theta}$. The nonlinear static functions $f_h(\cdot, \alpha)$ and $f_w(\cdot, \beta)$ in (4.1) and (4.3) represent general nonlinear functions.

In paper C and D, the Hammerstein and Wiener parts are each assumed to consist of one-dimensional polynomials stacks of orders $n_{h_i}$ and $n_{w_j}$, i.e.,

$$f_{h,i}(u_i, \alpha_i) = \alpha_{i,0} + \alpha_{i,1}u_i + ... + \alpha_{i,n_{h_i}}u_i^{n_{h_i}}, \text{ for } i = 1, \cdots, n_u, \tag{4.4}$$

and

$$f_{w,j}(z_j, \beta_j) = \beta_{j,0} + \beta_{j,1}z_j + ... + \beta_{j,n_{w_j}}z_j^{n_{w_j}}, \text{ for } j = 1, \cdots, n_y, \tag{4.5}$$

which implies that $h(t) \in \mathbb{R}^{n_u}$, and $z(t) \in \mathbb{R}^{n_y}$. The $j$th output $z_j(t)$ of the linear system $G(q, \theta)$ is given by

$$z_j(t) = \sum_{i=1}^{n_u} \frac{B_{j,i}(q)}{F_{j,i}(q)} h_i(t - n_{k_i}), \tag{4.6}$$

where $n_{k_i}$ is the input delay and the numerator and denominator polynomials, $B(q)$ and $F(q)$, are of the form

$$B_{j,i}(q) = b_1 + b_2q^{-1} + ... + b_{n_{b_{j,i}}}q^{-n_{b_{j,i}}+1} \tag{4.7}$$

and

$$F_{j,i}(q) = 1 + f_1 q^{-1} + f_2 q^{-2} + ... + f_{n_{f_{j,i}}} q^{-n_{f_{j,i}}}. \tag{4.8}$$

In (4.7) and (4.8), $n_{b_{j,i}}$ is the number of zeros plus 1, $n_{f_{j,i}}$ is the number of poles, and $q^{-1}$ is the backward shift operator.

The inputs are the two control valves commanded signals $V_u$ and $V_o$ and the inlet concentration $C_i$. The effect of $C_i$ was investigated in paper D and was found to improve the model fitness significantly. In Fig. 4.2, the resulting multiple-input single-output (MISO) Hammerstein-Wiener structure is shown, where $y_{OiW}$ represents the discharge concentration $C_u$, separation efficiency $\varepsilon_{red}$, and the discharge rate $Q_{u,oil}$.

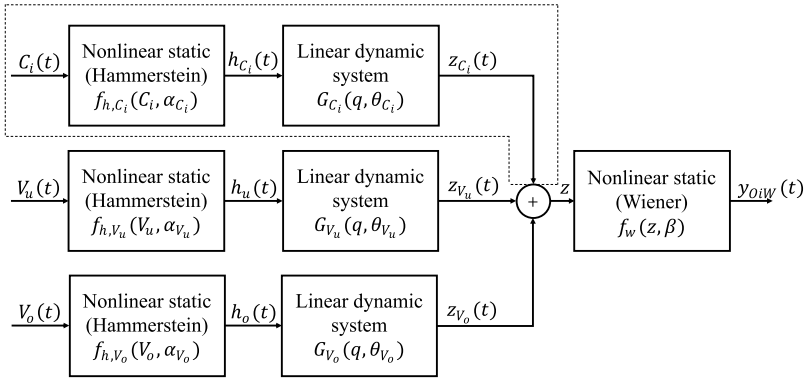


**Fig. 4.2:** The multiple-input single-output (MISO) HW model structure. The inputs $V_u$ and $V_o$ are the commanded valve positions, and $C_i$ is considered a measured input disturbance. The figure is from paper D.

Besides the model's coefficients, the orders of the static functions $n_h$ and $n_w$ need to be determined, as well as the TF model orders $n_b$, $n_f$, and system delay $n_k$. The identification problem can be posed as the minimization of the sum of squared prediction errors

$$\min_{\substack{\theta,\alpha,\beta \\ n_h,n_w,n_b,n_f,n_k}} \|y - \hat{y}\|_2^2 = \min_{\substack{\theta,\alpha,\beta \\ n_h,n_w,n_b,n_f,n_k}} \frac{1}{N} \sum_{t=1}^{N} \Big( y(t) - f_w(G(q,\theta) f_h(u(t),\alpha),\beta) \Big)^2, \tag{4.9}$$

where $N$ is the number of samples in the estimation data set.

Equation (4.9) is a mixed-integer minimization problem. To solve the problem, the delay $n_k$ was assumed to be a unit sample delay and an exhaustive search was used over the combination of model orders $n_h$, $n_w$, $n_b$, and $n_h$. For each combination of the model coefficients $\theta$, $\alpha$, and $\beta$ were found by

solving the simpler minimization

$$\min_{\theta,\alpha,\beta} \|y - \hat{y}\|_2^2 = \min_{\theta,\alpha,\beta} \frac{1}{N} \sum_{t=1}^{N} \Big( y(t) - f_w(G(q,\theta) f_h(u(t),\alpha),\beta) \Big)^2. \tag{4.10}$$

The solution to this minimization problem can be found through many optimization techniques. To solve it, MATLAB's System Identification Toolbox was used, which minimizes (4.10) through a combination of line search methods [74–79]. To reduce the number of model combinations, the following assumptions were used:

- All Hammerstein functions are given the same order;
- The TFs are required to be strictly proper, i.e., $n_b \leq n_f$;
- The delay $n_k$ is assumed to be the unit sample delay, i.e., $n_k = 1$.

### 4.1.1 System Identification Results

In this section, the identification results for modeling the separation efficiency are presented. HW models with polynomial Hammerstein and Wiener functions up to a 4th order, and TF orders up to a 3rd order were identified, corresponding to 5400 models. The models were compared to the validation data set and ordered based on their achieved normalized root mean square error (NRMSE) fitness

$$\text{NRMSE} = 100 \cdot \left( 1 - \frac{\|y - \hat{y}\|_2}{\|y - \overline{y}\|_2} \right) \%. \tag{4.11}$$

The model orders, number of variables, and NRMSE fitness of the five separation efficiency models with the highest fit to the validation data are given in Table 4.1.

**Table 4.1:** Models of separation efficiency with inputs $V_u$, $V_o$ and $C_i$. Model orders of Hammerstein function $n_h$, TF numerator polynomials $n_b$ and denominator polynomial $n_f$, Wiener function $n_w$, number of variables, estimation, and validation normalized root mean square error (NRMSE) fit and maximum steady-state efficiency. The table is from paper D.

| No. | $n_h$ | TF Model | $n_w$ | #var | *Est. Fit* [%] | *Val. Fit* [%] | *Max* $\epsilon$ [%] |
|---|---|---|---|---|---|---|---|
| 1 | 3 | $n_b$ = [1 1 2] $n_f$ = [2 2 3] | 0 | 23 | 78.25 | 64.16 | 61.10 |
| 2 | 2 | $n_b$ = [2 3 1] $n_f$ = [2 3 1] | 1 | 23 | 77.94 | 63.30 | 53.93 |
| 3 | 2 | $n_b$ = [2 3 1] $n_f$ = [2 3 3] | 1 | 25 | 78.03 | 63.20 | 53.93 |
| 4 | 3 | $n_b$ = [1 2 3] $n_f$ = [2 3 3] | 0 | 26 | 78.27 | 63.09 | 64.69 |
| 5 | 3 | $n_b$ = [1 1 2] $n_f$ = [3 2 3] | 0 | 24 | 78.36 | 63.00 | 65.05 |

The comparison between five selected models and the estimation and validation data are shown in Fig. 4.3 for the models of separation efficiency. The HW models fit reasonably well to the general shape of the data. Some smaller variations in the data are not captured by the models.

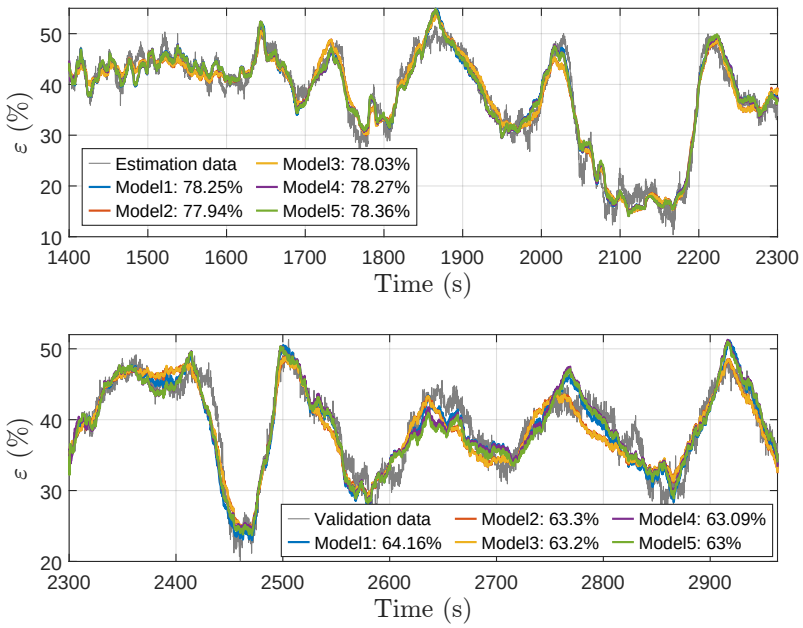


**Fig. 4.3:** Estimation data fit (top) and Validation fit (bottom) for the models from Table 4.1, with $V_u$, $V_o$ and $C_i$ as inputs.

The same was seen for the models of discharge concentration and discharge rate in paper D. The models of the discharge rate $Q_{u,oil}$ achieved a higher fitness to the data, but this can be explained by the strong correlation between $V_u$ and $Q_{u,oil}$, which made even linear models potential candidate models if model simplicity is preferred over model performance. Pure TF models did not perform well on the separation efficiency and discharge concentration data.

Besides the dynamic perspective, the steady-state surfaces of the three OiW outputs were examined over the input space of the control valves, as seen in Fig. 4.4 for model 1 in Table 4.1.

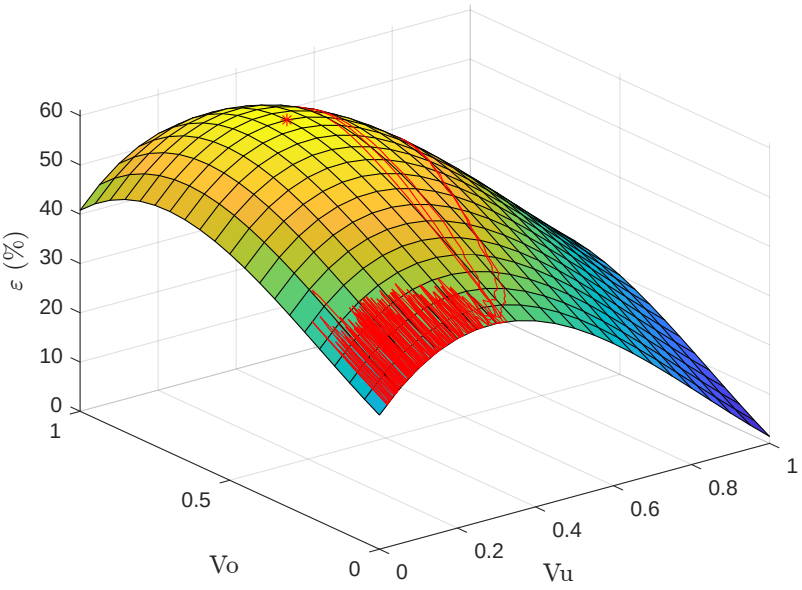


**Fig. 4.4:** Static efficiency surface of model 1 from Table 4.1, for fixed $C_i$. The valve travel from the estimation experiment is indicated with red lines, and the maximum efficiency is marked with a red asterisk. The figure is modified from paper D.

The surface in Fig. 4.4 indicates increasing separation efficiency with increasing $V_u$ at small opening degrees and deterioration of performance at larger valve openings, which is consistent with the observations seen in the identification experiment and the comparison study in chapter 3. The same tendency was observed for $V_o$, which was generally not expected but may result from the identification experiment, which only covered the valve combination corresponding to the red lines on the surface. Some suggestions to resolve these issues are given in paper D, such as opening the PDR loop to explore a larger portion of the input space.

The steady-state discharge concentration was seen to have the inverse shape of the separation efficiency curve as expected from (1.4). The steady-

state discharge rate was dominated by the effect of $V_u$, which indicates that control of $V_u$ plays a significant role in reducing the discharged oil volume.

## 4.2 Conclusion

A system identification approach was taken to obtain a model of the hydrocyclone separation dynamics. A methodology was proposed for identifying Hammerstein-Wiener models of de-oiling hydrocyclone separation efficiency, discharge rate, and discharge concentration. The identification experiment mimics an offshore PWT platform subjected to variable production, while the OiW concentrations are measured with online OiW monitors. The models capture the central dynamics of the data, and the steady-state surfaces describe the main mechanisms observed. Some regions of the steady-state surfaces are uncertain as they are extrapolations of the model. The limited exploration of the input space in the identification experiment is caused by the active level and PDR controller during the experiment.

With the obtained models, an OiW-based control design can be studied to investigate whether the separation performance of the PWT system can be improved with online OiW measurements.

# Chapter 5

# Control Based on Online Oil-in-Water Measurements

In chapter 3, the comparison of PDR-based controllers revealed that the MIMO controllers ($H_\infty$ and MPC) could mitigate the effect of flow rate disturbances $Q_{in}$ on PDR and separation efficiency, discharge rate, and discharge concentration. PDR did, however, not reflect the separation performance in all operating points. In chapter 4, nonlinear control-oriented models of separation efficiency, discharge rate, and discharge concentration were identified based on OiW measurements. In this chapter, two different control methods are used to design OiW-based controllers. In paper D, a PI-controller was designed using Skogestad internal model control (SIMC) tuning to track a discharge concentration reference. In paper E, a NMPC is designed to optimize the hydrocyclone separation efficiency. The controller naturally extends the existing PID-type PDR control as a cascaded control solution.

## 5.1 Skogestad Internal Model Control

In paper D, a PI controller was designed using the SIMC tuning method to directly control the discharge concentration, effectively replacing the PDR control loop. To obtain the SIMC-tuned PID controller, the model response to a step increase in $V_o$, which resembled a first-order response, was examined. The system step response was therefore approximated by a first-order plus dead time model, i.e.,

$$G(s) = \frac{k}{\tau_1 s + 1} e^{-\theta s}, \tag{5.1}$$

with time constant $\tau_1 = 24.4$ s, gain $k = -34.97$, and $\theta = 0.2$ s corresponding to a unit sample delay. For a first-order response, the tuning rules give a

series of PI-controller

$$c(s) = K_c \left(1 + \frac{1}{\tau_I s}\right). \tag{5.2}$$

The controller gains are given by

$$K_c = \frac{1}{k} \frac{\tau_1}{\tau_c + \theta} \tag{5.3}$$

and

$$\tau_I = min\{\tau_1, 4(\tau_c + \theta)\}, \tag{5.4}$$

where $\tau_c$ is the only tuning parameter. The minimum value of the controller time constant is $\tau_c = \theta$, resulting in a tight control setting. A value of $\tau_c = 14.15$ s was chosen to achieve a smoother control [80]. The closed-loop system was able to track a constant concentration reference, as seen in Fig. 5.1.

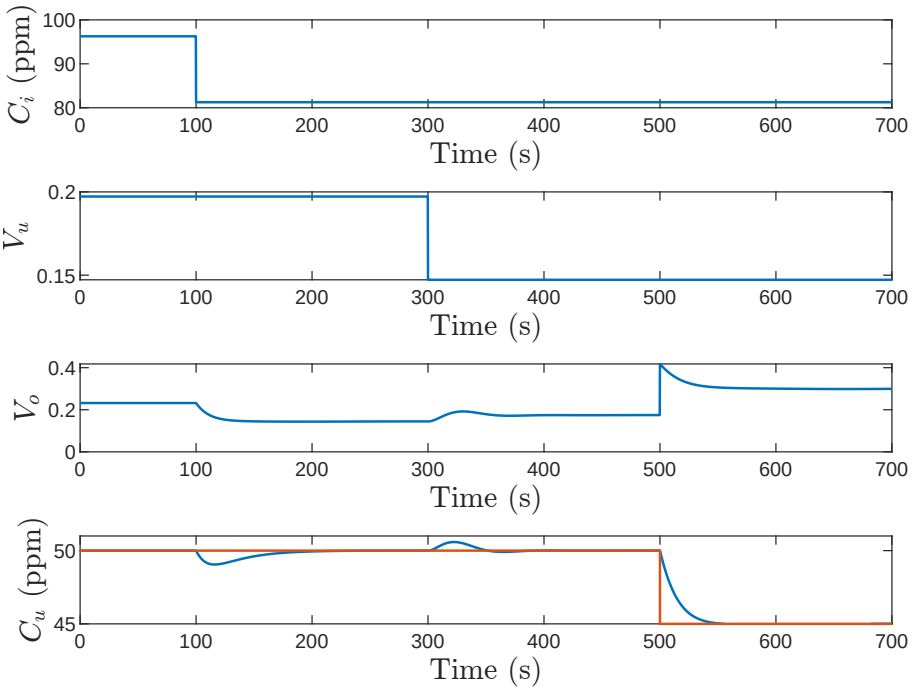


**Fig. 5.1:** Step responses of a HW model of the discharge concentration, subject to a decrease in inlet concentration $C_i$, a decrease in $V_u$, and change in reference. The figure is from paper D.

This represents one possible control solution by which the discharge concentration could be controlled to a reference below the legislative discharge limits. One drawback of this fixed reference controller occurs when the inlet concentration $C_i$ is reduced, resulting in a decrease in the discharge concentration $C_u$. To compensate for this behavior, the controller reduces the

opening degree of $V_o$ to increase $C_u$ back to the reference. Thus, due to the fixed reference, the system achieved suboptimal separation performance.

## 5.2 Nonlinear Model Predictive Control

The limitation of the obtained discharge concentration control in section 5.1 is the same as that of fixed reference PDR control, i.e., that the assigned reference may not be optimal. Additionally, the solution replaced the existing PDR controller directly. Although PDR does not directly measure the de-oiling separation efficiency, it still indirectly relates to the quality of the separated oil, i.e., the water content. Additionally, since PDR relies on pressure measurements, it can detect changing flow rates, and level controllers can be designed to mitigate flow disturbances, as seen in chapter 3.

A solution to these limitations was studied in paper E, where an NMPC was designed using the dynamic separation efficiency as the controlled variable. In the solution, the level control is unaltered while the designed NMPC controls the PDR reference to the existing PDR controller, as seen in Fig. 5.2.

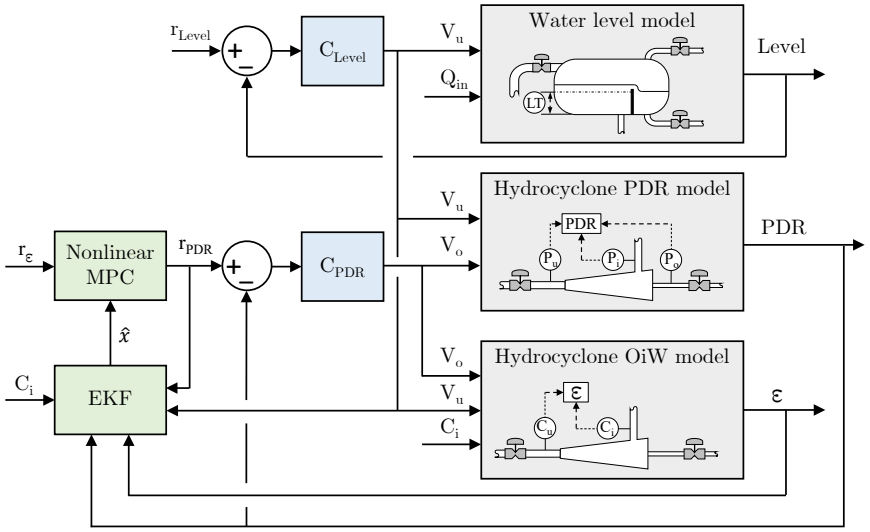


**Fig. 5.2:** Block diagram of the combined system model, where the nonlinear model predictive controller (NMPC) provides the PDR reference to the PDR controller $C_{PDR}$. The extended Kalman filter (EKF) estimates the prediction model states. The figure is from paper E.

Model 1 from Table 4.1 was combined with the models of separator oil-water interface level and PDR from section 3.1. The combined model was compared with the data from the identification experiment in paper C and D, which showed that the combined model captures the main dynamic features

of the data.

The prediction model for the NMPC consists of a PDR control loop with a PI controller $C_{PDR}$ and a PDR model (*Hydrocyclone PDR model*), as well as a separation efficiency model (*Hydrocyclone OiW model*) in Fig. 5.2. Building on top of the existing control structure has several advantages. As it was seen in chapter 2, the OiW monitors can be affected by many external conditions, such as fouling of the view cell, and the measurement may become unreliable. In this case, the OiW loop can be disconnected, and PDR-based control remains operational. The OiW measurement is typically also slower than the PDR measurement, and the cascaded solution allows the PDR controller to reject flow disturbances while the outer OiW loop mitigates OiW-related disturbances.

The proposed cost function is formulated as a trade-off between high separation efficiency and low flow split to separate as much oil as possible with high quality, i.e., low water content in the overflow. Instead of using flow split directly, the PDR can be used in the minimization of the cost function

$$J(k) = \sum_{i=1}^{H_p} \left( -w_1 \hat{y}_\varepsilon (k+i|k)^2 - \frac{w_2}{\hat{y}_{PDR}(k+i|k)^2} \right). \tag{5.5}$$

In (5.5), $\hat{y}_\varepsilon$ and $\hat{y}_{PDR}$ are the estimated separation efficiency and PDR respectively. As described in chapter 4, the separation efficiency model estimates an efficiency reduction in the upper range of $V_o$, which is generally unexpected. Therefore, using PDR in the cost function was unnecessary, and the applied cost function utilized $w_1 = 1$ and $w_2 = 0$ to optimize the separation efficiency directly.

Filtered data of the inlet concentration $C_i$ and the production flow rate $Q_{in}$ was used in the simulation. Gaussian noise was added to the measurements used by the NMPC, i.e., the inlet concentration $C_i$, PDR, and separation efficiency $\varepsilon$. The noise variances were found based on measured data from the testing facility. Although the PDR was reduced from the cost function, it was used for the state estimation using an extended Kalman filter.

Figure 5.3 shows the comparison between the PID solution from section 3.2, representing the existing control solution and the NMPC. The PID controller failed to keep PDR at the reference, and the PDR varies due to the changing flow rate disturbance $Q_{in}$ and the strict level control, which transfers the disturbance to the PDR loop. Instead, the NMPC varies the PDR reference to steer $V_o$ to the optimum opening degree. As seen in Fig. 5.3, the separation efficiency is higher during the simulation scenario when using the NMPC. The mean separation efficiency was 11.7 percentage points larger than the efficiency of the PID controller, while simultaneously actuating the overflow valve was 95.6% less than the PID, thereby reducing wear.

The separation efficiency was defined as the control variable in this work,

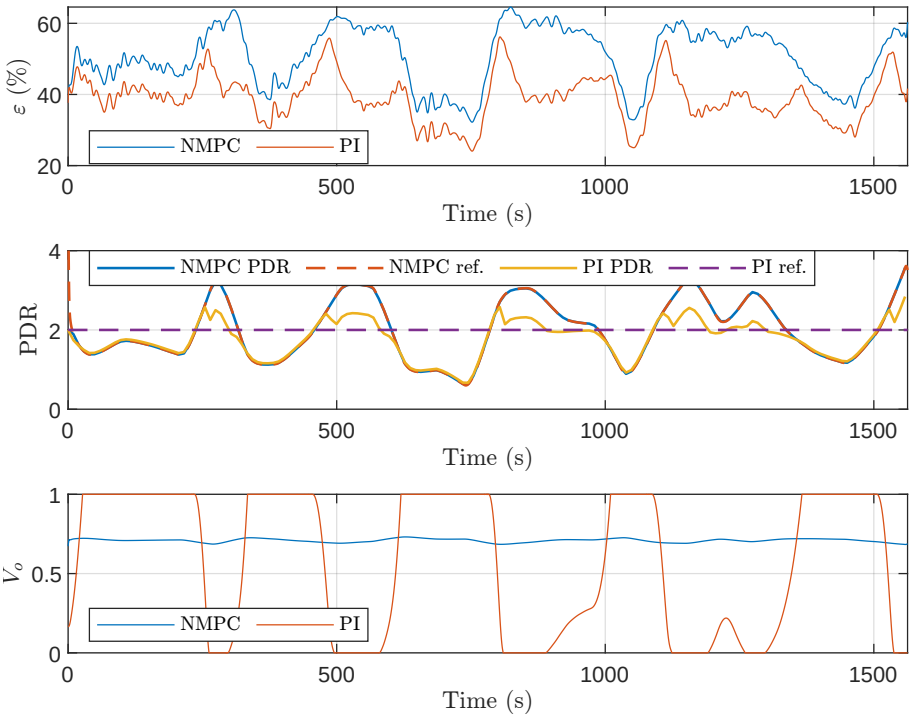


**Fig. 5.3:** The separation efficiency $\varepsilon$ achieved with the PDR-based PI controller and the NMPC controlling separation efficiency (top), the PDR and PDR-references (middle), and the actuation of the overflow valve $V_o$ (bottom). The figure is from paper E.

but the same solution could be applied with discharge concentration or discharge rate. As $V_o$ mainly affects $C_u$, minimization of the discharge concentration is equivalent to maximization of the separation efficiency from the definition of $\varepsilon_{red}$ in (1.4). This is also observed from the steady-state plots of discharge concentration and separation efficiency in paper D. The same should be the case for the discharge rate, as the controller examined here only influences $Q_u$ to a small degree on an offshore PWT facility.

## 5.3 Conclusion

A SIMC-tuned PI controller was designed to replace the PDR-based control and directly control the discharge concentration to a fixed reference. However, a fixed reference does not guarantee optimal system performance since the controller actuates $V_o$ to track the reference even when the discharge concentration is below the reference. As an alternative, a NMPC was designed to optimize the hydrocyclone separation efficiency. The NMPC extends the

existing control structure by generating the reference to the PDR controller to actively keep the separation efficiency near the optimum. The NMPC significantly improved the separation efficiency and reduced the actuation of $V_o$, leading to less valve wear. While the combined plant model does describe the main dynamics of the system, the control solution still needs to be tested experimentally. In the separation efficiency model, the efficiency is reduced at large $V_o$, which is generally unexpected. In the real system, a trade-off between maximum separation efficiency and PDR could be made to achieve high separation efficiency and low water content in the separated oil. Although the improvements might be smaller in reality, the results indicate that such a control solution could be a feasible way to include the OiW-based control while keeping the advantages of the existing PDR control.

# Chapter 6

# Closing remarks

With the global increase in energy demand, offshore oil production is expected to continue in the coming decades, with large quantities of produced water (PW) discharged into the ocean. The main objective of this thesis was to investigate whether online oil-in-water (OiW) monitors can be used to improve the de-oiling performance of offshore produced water treatment (PWT) systems to reduce the discharge of oil to the marine environment.

The main contributions of this work can be summarized as:

- Investigation of challenges related to the application of OiW monitors.
- Performance comparisons of advanced pressure drop ratio (PDR) controllers using OiW monitors.
- Analysis of alternative OiW-related controlled variables, such as the discharge rate.
- Methodology to obtain nonlinear control-oriented models of de-oiling hydrocyclones using OiW monitors.
- Nonlinear model predictive controller (NMPC) that optimizes separation efficiency cascaded with the conventional PDR-based proportional integral derivative (PID) solution commonly used on offshore PWT facilities.

UV-fluorescence monitors were used throughout this work to measure the OiW concentration. Preparations and tests of different process conditions on the UV-fluorescence monitors were carried out in paper A. Based on the results, improvements were implemented in the sidestream sampling section of the testing facility.

OiW monitors were used to compare the performance of some advanced PDR-based control solutions against the industry standard PID control solution in paper B. The experiment mimics an offshore PWT facility subjected to variable production rates. The separation efficiency, oil discharge rate, and discharge concentration were used for the comparison, as well as the accumulated values of oil production, separated water, and oil discharge. The model predictive controller (MPC) performed the best overall, but the performance of the MPC and the robust $H_\infty$ controller were similar. The improved performance of the advanced controllers is generally attributed to the relaxation of the level control, which, as intended, stabilizes the inlet flow rate to the hydrocyclone and effectively reduces variations in the separation. It was observed that the fixed reference of PDR does not correspond to optimal separation in all operating points, which motivates control based on OiW monitors. The comparison also revealed that a high separation efficiency and low discharge concentration can still result in a large discharge rate, as both the separation efficiency and discharge rate are positively correlated with the inlet flow rate within a range. Therefore, potential multiple-input multiple-output (MIMO) control solutions must consider the combined separation efficiency of the three-phase separator tank and hydrocyclone system or consider the discharge flow rate. One way to consider the total discharge performance is to use the discharge rate as the controlled variable, as it considers the discharge concentration and flow together.

A system identification approach to model the hydrocyclone separation efficiency was presented in paper C. The identification experiment was similar to the PID experiment in paper B emulating an offshore PWT facility with installed OiW monitors subjected to variable production rates. Hammerstein-Wiener models were proposed and identified with reasonable results on the obtained data. The model performance was deemed acceptable for the control design. However, some of the outer regions of the examined steady-state surfaces seem less realistic, which might be due to the identification experiment. Some suggestions for improvements were given in paper D. The methodology was extended in paper D to modeling of the discharge concentration and discharge rate. The obtained models only required knowledge about the inlet and discharge concentration and the commanded control valve opening degrees. The advantage of the system identification experiment is that, in principle, historical data could be available with the legislative requirements to install OiW monitors for reporting oil discharges. To demonstrate the models, a PI controller was tuned using the Skogestad internal model control (SIMC) method to control the discharge concentration. The results show that the model could reject disturbances in inlet flow rate and inlet concentration. Meanwhile, it was able to track a discharge concentration reference, which could be a potential control variable instead of PDR.

The conventional PID-type PDR control was extended with a NMPC in

paper E. Instead of a fixed PDR reference, the NMPC provides the PDR reference to the PDR control loop to optimize the dynamic separation efficiency. The simulation results show a promising increase in separation efficiency and reduced valve wear compared with the conventional PID control. These results indicate that such an approach might be feasible, but experimental testing is needed to validate the approach. The dynamic separation efficiency is used as it directly explains the hydrocyclone performance. However, as the control of the overflow valve mainly affects the hydrocyclone performance, the discharge concentration or oil discharge rate studied could be equally applied.

In future work, this approach can be extended to include control of the water level in the three-phase separator to improve the separation performance further. However, such an approach must consider the combined system performance and the balance between performance and production.

Based on the results from paper A–E, this thesis has demonstrated feedback control solutions that utilize online OiW monitors to optimize oil separation from PW in PWT facilities. The presented solution acts as a layer on top of the existing hydrocyclone control loop, allowing the operator to switch between the traditional PDR-based control and the extended version based on online OiW measurements. If the proposed methods show similar results on actual PWT facilities, tonnes of oil will be separated instead of discharged to the marine environment.

# References


[1] EIA, "International Energy Outlook 2023," U.S. Energy Information Administration, Washington, DC, USA, Tech. Rep., pp. 1–64, 2023.

[2] IEA, "World Energy Outlook 2022," International Energy Agency, Paris, France, Tech. Rep., pp. 1–524, 2022.

[3] U. Ahmed, "Making the Most of Maturing Fields," *Oilfield Review*. Schlumberger, 2004, vol. 16, no. 2, pp. 1–1, 2004.

[4] Danish Energy Agency, "Ressourceropgørelse og prognoser," Danish Energy Agency, Copenhagen, Denmark, Tech. Rep., pp. 1–9, 2018.

[5] DEA, "Monthly and Yearly Production," Copenhagen, Denmark, 2022. [Online]. Available: https://ens.dk/en/our-services/oil-and-gas-related-data/monthly-and-yearly-production (Accessed 2023-10-19).

[6] F. Brette, B. Machado, C. Cros, J. P. Incardona, N. L. Scholz, and B. A. Block, "Crude Oil Impairs Cardiac Excitation-Contraction Coupling in Fish," *Science*. AAAS, 2014, vol. 343, no. 6172, pp. 772–776, 2014. Doi: 10.1126/science.1242747

[7] OSPAR, "OSPAR Recommendation 2001/1 for the Management of Produced Water from Offshore Installations," OSPAR Commission, London, UK, Tech. Rep., pp. 1–8, 2001.

[8] OSPAR, "Assessment of the impacts of the offshore oil and gas industry on the marine environment," OSPAR Commission, London, UK, Tech. Rep., pp. 1–56, 2022.

[9] Danish Environmental Protection Agency, "Generel tilladelse for Total E&P Danmark A/S ( TOTAL ) til anvendelse , udled- ning og anden bortskaffelse af stoffer og materialer , herunder olie og kemikalier i produktions- og injektionsvand fra produktionsenhederne Halfdan , Dan , Tyra og Gorm," Danish Environmental Protection Agency, Copenhagen, Denmark, Tech. Rep., pp. 1–12, 2018.

[10] OSPAR, "OSPAR Discharges, Spills and Emissions from Offshore Oil and Gas Installations - 2020," London, UK, 2021. [Online]. Available: https://odims.ospar.org/en/submissions/ospar_discharges_offshore_2020_01/ (Accessed 2023-01-25).

[11] E. Blanchard, "Oil in Water Monitoring is a Key to Production Separation," *Offshore*. Endeavor Business Media, 2013, vol. 73, no. 11, pp. 104–105, 2013.

[12] L. Jin and A. K. Wojtanowicz, "Progression of injectivity damage with oily waste water in linear flow," *Petroleum Science*. Springer, 2014, vol. 11, no. 4, pp. 550–562, 2014. Doi: 10.1007/s12182-013-0371-0

[13] N. Zhang, J. Somerville, and A. Todd, "An Experimental Investigation of the Formation Damage Caused by Produced Oily Water Injection," in Proceedings of *Offshore Europe*. Society of Petroleum Engineers, 1993, pp. 265–274. Doi: 10.2118/26702-MS

[14] J. M. Walsh, "Produced-Water-Treating Systems: Comparison of North Sea and Deepwater Gulf of Mexico," *Oil and Gas Facilities*. Society of Petroleum Engineers, 2015, vol. 4, no. 2, pp. 73–86, 2015. Doi: 10.2118/159713-PA

[15] M. V. Bram, S. Jespersen, D. S. Hansen, and Z. Yang, "Control-Oriented Modeling and Experimental Validation of a Deoiling Hydrocyclone System," *Processes*. MDPI, 2020, vol. 8, no. 9, pp. 1–33, 2020. Doi: 10.3390/pr8091010

[16] M. F. Schubert, F. Skilbeck, and H. J. Walker, "Liquid hydrocyclone separation systems," in *Hydrocyclones: Analysis and Applications*, 1st ed., L. Svarovsky and M. T. Thew, Eds. Springer, 1992, pp. 275–293. Doi: 10.1007/978-94-015-7981-0_18

[17] W. J. Georgie, "Effective and Holistic Approach to produced Water Management for Offshore Operation," in Proceedings of *Offshore Technology Conference*. Houston, TX, USA: Society of Petroleum Engineers, 2002, pp. 2527–2539. Doi: 10.4043/14286-ms

[18] A. F. Sayda and J. H. Taylor, "Modeling and Control of Three-Phase Gravity Separators in Oil Production Facilities," in Proceedings of *2007 American Control Conference*. New York, NY, USA: IEEE, 2007, pp. 4847–4853. Doi: 10.1109/ACC.2007.4282265

[19] C. J. Backi and S. Skogestad, "A simple dynamic gravity separator model for separation efficiency evaluation incorporating level and pressure control," in Proceedings of *2017 American Control Conference (ACC)*. Seattle, WA, USA: IEEE, 2017, pp. 2823–2828. Doi: 10.23919/ACC.2017.7963379

[20] J. M. Stinson, "The hydrocyclone - a story of continuous innovation," in *Hydrocyclones: Analysis and Applications*, 1st ed., L. Svarovsky and M. T. Thew, Eds. Springer Netherlands, 1992, pp. i–iv. Doi: https://doi.org/10.1007/978-94-015-7981-0

[21] Y. Liu, Q. Cheng, B. Zhang, and F. Tian, "Three-phase hydrocyclone separator – A review," *Chemical Engineering Research and Design*. Elsevier, 2015, vol. 100, no. 8, pp. 554–560, 2015. Doi: 10.1016/j.cherd.2015.04.026

[22] A. K. Wojtanowicz, *Environmental Control of Drilling Fluids and Produced Water*, 3rd ed. Springer, 2016, ch. 2, pp. 101–165. Doi: 10.1007/978-3-319-24334-4_4

[23] J. A. Veil, *Produced Water Management Options and Technologies*, 1st ed. Springer, 2011, ch. 29, pp. 537–571. Doi: 10.1007/978-1-4614-0046-2_29

[24] D. S. Hansen, S. Jespersen, M. V. Bram, and Z. Yang, "Uncertainty Analysis of Fluorescence-Based Oil-In-Water Monitors for Oil and Gas Produced Water," *Sensors*. MDPI, 2020, vol. 20, no. 16, pp. 1–36, 2020. Doi: 10.3390/s20164435

[25] M. S. Choi, "Hydrocyclone produced water treatment for offshore developments," in Proceedings of *SPE Annual Technical Conference and Exhibition*. New Orleans, LA, USA: Society of Petroleum Engineers, 1990, pp. 473–480. Doi: 10.2118/20662-MS

[26] P. S. Jones, "A field comparison of static and dynamic hydrocyclones," *SPE Production & Facilities*. SPE, 1993, vol. 8, no. 2, pp. 84–90, 1993. Doi: 10.2118/20701-PA

[27] A. B. Sinker, M. Humphris, and N. Wayth, "Enhanced Deoiling Hydrocyclone Performance without Resorting to Chemicals," in Proceedings of *SPE Offshore Europe Oil and Gas Conference and Exhibition*. Aberdeen,UK: Society of Petroleum Engineers, 1999, pp. 1–9. Doi: 10.2118/56969-MS

[28] J. Coca-Prados, G. Gutiérrez-Cervelló, and J. M. Benito, *Treatment of Oily Wastewater*, 1st ed., ser. NATO Science for Peace and Security Series C: Environmental Security. Springer, 2011, ch. 1, pp. 1–55. Doi: 10.1007/978-90-481-9775-0_1

[29] D. A. Colman and M. T. Thew, "Correlation of separation results from light dispersion hydrocyclones," *Chemical Engineering Research & Design*. Institution of Chemical Engineers, 1983, vol. 61, no. 4, pp. 233–240, 1983.

[30] L. Svarovsky and J. Svarovsky, "A new method of testing hydrocyclone grade efficiencies," in *Hydrocyclones: Analysis and Applications*, 1st ed., L. Svarovsky and M. T. Thew, Eds. Springer, 1992, pp. 135–145. Doi: 10.1007/978-94-015-7981-0_10

[31] D. S. Hansen, M. V. Bram, and Z. Yang, "Efficiency investigation of an offshore deoiling hydrocyclone using real-time fluorescence- and microscopy-based monitors," in Proceedings of *2017 IEEE Conference on Control Technology and Applications (CCTA)*. Maui, HI, USA: IEEE, 2017, pp. 1104–1109. Doi: 10.1109/CCTA.2017.8062606

[32] T. Husveg, O. Rambeau, T. Drengstig, and T. Bilstad, "Performance of a deoiling hydrocyclone during variable flow rates," *Minerals Engineering*. Pergamon, 2007, vol. 20, no. 4, pp. 368–379, 2007. Doi: 10.1016/j.mineng.2006.12.002

[33] N. Meldrum, "Hydrocyclones: A Solution to Produced-Water Treatment," *SPE Production Engineering*. SPE, 1988, vol. 3, no. 4, pp. 669–676, 1988. Doi: 10.2118/16642-PA

[34] M. T. Thew, "FLOTATION | Cyclones for Oil/Water Separations," in *Encyclopedia of Separation Science*, 1st ed., I. Wilson, C. Poole, and M. Cooke, Eds. Elsevier, 2000, pp. 1480–1490. Doi: http://dx.doi.org/10.1016/B0-12-226770-2/04601-9

[35] G. Young, W. Wakley, D. Taggart, S. Andrews, and J. Worrell, "Oil-water separation using hydrocyclones: An experimental search for optimum dimensions," *Journal of Petroleum Science and Engineering*. Elsevier, 1994, vol. 11, no. 1, pp. 37–50, 1994. Doi: 10.1016/0920-4105(94)90061-2

[36] N. Kharoua, L. Khezzar, and Z. Nemouchi, "Computational fluid dynamics study of the parameters affecting oil—water hydrocyclone performance," *The Institution of Mechanical Engineers, Part E: Journal of Process Mechanical Engineering*. SAGE Publications, 2010, vol. 224, no. 2, pp. 119–128, 2010. Doi: 10.1243/09544089JPME304

[37] Y. R. Murthy and K. U. Bhaskar, "Parametric CFD studies on hydrocyclone," *Powder Technology*. Elsevier, 2012, vol. 230, pp. 36–47, 2012. Doi: 10.1016/j.powtec.2012.06.048

[38] P. Durdevic, S. Pedersen, and Z. Yang, "Operational performance of offshore de-oiling hydrocyclone systems," in Proceedings of *IECON 2017 - 43rd Annual Conference of the IEEE Industrial Electronics Society*. Beijing, China: IEEE, 2017, pp. 6905–6910. Doi: 10.1109/IECON.2017.8217207

[39] Zhenyu Yang, S. Pedersen, and P. Durdevic, "Cleaning the produced water in offshore oil production by using plant-wide optimal control strategy," in Proceedings of *2014 Oceans - St. John's*. IEEE, 2014, pp. 1–10. Doi: 10.1109/OCEANS.2014.7003038

[40] P. Durdevic and Z. Yang, "Application of $H_\infty$ Robust Control on a Scaled Offshore Oil and Gas De-Oiling Facility," *Energies*. MDPI, 2018, vol. 11, no. 2, pp. 1–18, 2018. Doi: 10.3390/en11020287

[41] L. Hansen, P. Durdevic, K. L. Jepsen, and Z. Yang, "Plant-wide Optimal Control of an Offshore De-oiling Process Using MPC Technique," *IFAC-PapersOnLine*. Elsevier, 2018, vol. 51, no. 8, pp. 144–150, 2018. Doi: 10.1016/j.ifacol.2018.06.369

[42] M. V. Bram, A. A. Hassan, D. S. Hansen, P. Durdevic, S. Pedersen, and Z. Yang, "Experimental modeling of a deoiling hydrocyclone system," in Proceedings of *2015 20th International Conference on Methods and Models in Automation and Robotics (MMAR)*. Miedzyzdroje, Poland: IEEE, 2015, pp. 1080–1085. Doi: 10.1109/MMAR.2015.7284029

[43] P. Durdevic, S. Pedersen, M. Bram, D. Hansen, A. Hassan, and Z. Yang, "Control Oriented Modeling of a De-oiling Hydrocyclone," *IFAC-PapersOnLine*. Elsevier, 2015, vol. 48, no. 28, pp. 291–296, 2015. Doi: 10.1016/j.ifacol.2015.12.141

[44] M. Vallabhan K.G., C. Holden, and S. Skogestad, "Deoiling Hydrocyclones: An Experimental Study of Novel Control Schemes," *SPE Production & Operations*. SPE, 2022, vol. 37, no. 3, pp. 462–474, 2022. Doi: 10.2118/209576-PA

[45] M. K. Vallabhan, J. Matias, and C. Holden, "Feedforward, cascade and model predictive control algorithms for de-oiling hydrocyclones: simulation study," *Modeling, Identification and Control*. Norwegian Society of Automatic Control, 2021, vol. 42, no. 4, pp. 185–195, 2021. Doi: 10.4173/mic.2021.4.4

[46] M. Yang, *Measurement of Oil in Produced Water*, 1st ed. Springer, 2011, ch. 2, pp. 57–88. Doi: 10.1007/978-1-4614-0046-2_2

[47] R. M. Van der Heul, "Environmental Degradation of petroleum hydrocarbons," Utrecht University, Utrecht, Netherlands, Tech. Rep., pp. 1–53, 2009.

[48] D. L. Gallup, *Advances in Oil-in-Water Monitoring Technology*, 1st ed. CRC Press, 2015, ch. 3, pp. 51–58. Doi: 10.1201/b18109-6

[49] Turner Designs Hydrocarbon Instruments, "E09 TD-4100XDC Oil in Water Monitor User Manual," Turner Designs, Fresno, CA, Tech. Rep., pp. 1–272, 2014.

[50] A. Motin, V. V. Tarabara, C. A. Petty, and A. Bénard, "Hydrodynamics within flooded hydrocyclones during excursion in the feed rate: Understanding of turndown ratio," *Separation and Purification Technology*. Elsevier, 2017, vol. 185, pp. 41–53, 2017. Doi: 10.1016/j.seppur.2017.05.015

[51] S. Noroozi and S. Hashemabadi, "CFD analysis of inlet chamber body profile effects on de-oiling hydrocyclone efficiency," *Chemical Engineering Research and Design*. Institution of Chemical Engineers, 2011, vol. 89, no. 7, pp. 968–977, 2011. Doi: 10.1016/j.cherd.2010.11.017

[52] A. Motin and A. Bénard, "Design of liquid–liquid separation hydrocyclones using parabolic and hyperbolic swirl chambers for efficiency enhancement," *Chemical Engineering Research and Design*. Elsevier, 2017, vol. 122, pp. 184–197, 2017. Doi: 10.1016/j.cherd.2017.04.012

[53] M. Durango-Cogollo, J. Garcia-Bravo, B. Newell, and A. Gonzalez-Mancera, "CFD Modeling of Hydrocyclones—A Study of Efficiency of Hydrodynamic

Reservoirs," *Fluids*. MDPI, 2020, vol. 5, no. 3, pp. 1–19, 2020. Doi: 10.3390/fluids5030118

[54] K. U. Bhaskar, Y. R. Murthy, M. R. Raju, S. Tiwari, J. K. Srivastava, and N. Ramakrishnan, "CFD simulation and experimental validation studies on hydrocyclone," *Minerals Engineering*. Elsevier, 2007, vol. 20, no. 1, pp. 60–71, 2007. Doi: 10.1016/j.mineng.2006.04.012

[55] D. Wolbert, B. F. Ma, Y. Aurelle, and J. Seureau, "Efficiency estimation of liquid-liquid Hydrocyclones using trajectory analysis," *AIChE Journal*. Wiley, 1995, vol. 41, no. 6, pp. 1395–1402, 1995. Doi: 10.1002/aic.690410606

[56] S. Amini, D. Mowla, M. Golkar, and F. Esmaeilzadeh, "Mathematical modelling of a hydrocyclone for the down-hole oil-water separation (DOWS)," *Chemical Engineering Research and Design*. Elsevier, 2012, vol. 90, no. 12, pp. 2186–2195, 2012. Doi: 10.1016/j.cherd.2012.05.007

[57] J. Caldenley, C. Gomez, S. Wang, L. Gomez, R. Mohan, and O. Shoham, "Oil/water separation in liquid/liquid hydrocyclones (llhc): Part 2 - mechanistic modeling," *SPE Journal*. SPE, 2002, vol. 7, no. 4, pp. 362–372, 2002. Doi: 10.2118/81592-PA

[58] M. K. G. Vallabhan, C. Holden, and S. Skogestad, "A First-Principles Approach for Control-Oriented Modeling of De-oiling Hydrocyclones," *Industrial & Engineering Chemistry Research*. American Chemical Society, 2020, vol. 59, no. 42, pp. 18 937–18 950, 2020. Doi: 10.1021/acs.iecr.0c02859

[59] M. V. Bram, L. Hansen, D. S. Hansen, and Z. Yang, "Extended Grey-Box Modeling of Real-Time Hydrocyclone Separation Efficiency," in Proceedings of *2019 18th European Control Conference (ECC)*. Naples, Italy: IEEE, 2019, pp. 3625–3631. Doi: 10.23919/ECC.2019.8796175

[60] H. Sivertsen, E. Storkaas, and S. Skogestad, "Small-scale experiments on stabilizing riser slug flow," *Chemical Engineering Research and Design*. Elsevier, 2010, vol. 88, no. 2, pp. 213–228, 2010. Doi: 10.1016/j.cherd.2009.08.007

[61] P. Durdevic and Z. Yang, "Dynamic Efficiency Analysis of an Off-Shore Hydrocyclone System Subjected to a Conventional PID- and Robust-Control-Solution," *Energies*. MDPI, 2018, vol. 11, no. 9, pp. 1–14, 2018. Doi: 10.3390/en11092379

[62] S. Pedersen, "Plant-Wide Anti-Slug Control for Offshore Oil and Gas Processes," Ph.D. Thesis, Aalborg University, Aalborg, Denmark, 2016. Doi: 10.5278/vbn.phd.engsci.00183

[63] P. Durdevic, "Real-Time Monitoring and Robust Control of Offshore De-oiling Processes," Ph.D. Thesis, Aalborg University, Aalborg, Denmark, 2017.

[64] D. S. Hansen, "Online Monitoring and Analysis of Water Quality in Offshore Oil & Gas Production," Ph.D. Thesis, Aalborg University, Aalborg, Denmark, 2021. Doi: 10.5278/vbn.phd.eng.00080

[65] K. L. Jepsen, "Modeling and Control of Membrane Filtration Systems for Offshore Produced Water Treatment," Ph.D. Thesis, Aalborg University, Aalborg, Denmark, 2019. Doi: 10.54337/aau311246781

[66] M. V. Bram, "Grey-Box Modeling and Validation of Deoiling Hydrocyclones," Ph.D. Thesis, Aalborg University, Aalborg, Denmark, 2020.

[67] Midland, "Midland Non Detergent 30," Midland, Hunzenschwil, Switzerland, Tech. Rep., pp. 1–2, 2011.

[68] S. Kumar Panigrahi and A. Kumar Mishra, "Inner filter effect in fluorescence spectroscopy: As a problem and as a solution," *Journal of Photochemistry and Photobiology C: Photochemistry Reviews*. Elsevier, 2019, vol. 41, no. 12, pp. 1–28, 2019. Doi: 10.1016/j.jphotochemrev.2019.100318

[69] J. R. Lakowicz, *Principles of fluorescence spectroscopy*, 3rd ed. Springer, 2006. Doi: 10.1007/978-0-387-46312-4

[70] K. Zhou, J. C. Doyle, and K. Glover, *Robust and optimal control*, 1st ed. Upper Saddle River, N.J: Prentice Hall, 1996.

[71] J. Zhang, Z. Tang, M. Ai, and W. Gui, "Nonlinear modeling of the relationship between reagent dosage and flotation froth surface image by Hammerstein-Wiener model," *Minerals Engineering*. Elsevier, 2018, vol. 120, pp. 19–28, 2018. Doi: 10.1016/j.mineng.2018.01.018

[72] E. Atam, D. O. Schulte, A. Arteconi, I. Sass, and L. Helsen, "Control-oriented modeling of geothermal borefield thermal dynamics through Hammerstein-Wiener models," *Renewable Energy*. Elsevier, 2018, vol. 120, pp. 468–477, 2018. Doi: 10.1016/j.renene.2017.12.105

[73] D. Copaci, L. Moreno, and D. Blanco, "Two-Stage Shape Memory Alloy Identification Based on the Hammerstein–Wiener Model," *Frontiers in Robotics and AI*. Frontiers Media, 2019, vol. 6, pp. 1–10, 2019. Doi: 10.3389/frobt.2019.00083

[74] L. Ljung, "System Identification Toolbox User's Guide," The Mathworks, Inc, Massachusetts, USA, Tech. Rep., pp. 12–1 – 12–30, 2022.

[75] L. Ljung, Q. Zhang, P. Lindskog, A. Iouditski, and R. Singh, "An integrated system identification toolbox for linear and non-linear models," *IFAC Proceedings Volumes*. Elsevier, 2006, vol. 39, pp. 931–936, 2006. Doi: 10.3182/20060329-3-AU-2901.00148

[76] L. Ljung, R. Singh, Q. Zhang, P. Lindskog, and A. Iouditski, "Developments in the mathworks system identification toolbox," *IFAC Proceedings Volumes*. Elsevier, 2009, vol. 42, pp. 522–527, 2009. Doi: 10.3182/20090706-3-FR-2004.00086

[77] A. Wills, T. B. Schön, L. Ljung, and B. Ninness, "Identification of Hammerstein–Wiener models," *Automatica*. Elsevier, 2013, vol. 49, no. 1, pp. 70–81, 2013. Doi: 10.1016/j.automatica.2012.09.018

[78] A. Hagenblad, L. Ljung, and A. Wills, "Maximum Likelihood Identification of Wiener Models," *IFAC Proceedings Volumes*. Elsevier, 2008, vol. 41, no. 2, pp. 2714–2719, 2008. Doi: 10.3182/20080706-5-KR-1001.00457

[79] L. Ljung, *System Identification: Theory for the User*, 2nd ed., ser. Prentice Hall information and system sciences series. Prentice Hall PTR, 1999.

[80] S. Skogestad, "Simple analytic rules for model reduction and PID controller tuning," *Modeling, Identification and Control: A Norwegian Research Bulletin*. Norwegian Society of Automatic Control, 2004, vol. 25, no. 2, pp. 85–120, 2004. Doi: 10.4173/mic.2004.2.2

ISSN (online): 2446-1636
ISBN (online): 978-87-7573-601-0

AALBORG UNIVERSITY PRESS